Electronic Supplementary Information (ESI) for

Azophotoswitches containing thiazole, isothiazole, thiadiazole and isothiadiazole

Nusaiba Madappuram Cheruthu, [a,b] P. K. Hashim, [a,b] Saugata Sahu,[a] Kiyonori Takahashi,[a] Takayoshi Nakamura,[a,c] Hideyuki Mitomo,[a,b] Kuniharu Ijiro[a,b] and Nobuyuki Tamaoki *[a,b]

[a]*Research Institute for Electronic Science, Hokkaido University, Kita 20, Nishi 10, Kita-ku, Sapporo, Hokkaido, 001-0020, Japan.*

[b]*Graduate School of Life Science, Hokkaido University, Kita 10, Nishi 8, Kita-ku, Sapporo, Hokkaido, 060-0810, Japan.*

[c]*Department of Chemistry, Graduate School of Advanced Science and Engineering, Hiroshima University, Higashi-hiroshima 739-8526, Japan*

Correspondence should be addressed to N. T. (E-mail: tamaoki@es.hokudai.ac.jp)

Table of contents

1. Experimental and instrumentation methods

Chemicals: All reagents and solvents were purchased from commercial sources (FUJIFILM Wako Pure Chemical Corporation, Tokyo Chemical Industry, Merck, Kanto Chemical) and used without further purification.

Instrumentation: Reactions progress was monitored using thin-layer chromatography with TLC silica gel 60 F_{254} (Merck). Column chromatography was performed using silica gel 60 N (spherical, neutral, 40-50 μm, 63-210 μm, Kanto chemical). NMR spectra (^{1}H, ^{13}C) were measured by a JEOL ECX-400 (400 or 600 MHz) spectrometer. A Shimadzu UV spectrophotometer (UV-1800) equipped with a TCC-100 Shimadzu temperature-controlled cell holder was used for UV-vis spectrophotometry. Photoisomerization studies were carried out using a LED light source (Asahi Spectra, CL-1503) with LED heads emitting at 365 nm, 405 nm, 430 nm, 470 nm, 525 nm, and 568 nm. The absorption spectra of the fast-switching compounds **4** and **6** were acquired using an Agilent 8453 spectrophotometer under continuous irradiation at specific wavelengths. Each sample was irradiated unilaterally in the cuvette, and spectra were recorded during irradiation once the photostationary state (PSS) was reached. For compound **4**, irradiation was maintained at 405 nm for *trans*-to-*cis* isomerization, followed by 525 nm for the *cis*-to-*trans* conversion. Similarly, compound **6** was continuously irradiated at 430 nm for *trans*-to-*cis* isomerization and at 568 nm for the *cis*-to-*trans* reversion while recording absorption spectra.

2. Screening λ_{max} of the photoswitches by DFT calculations

DFT calculations were performed on 24 photoswitchable molecules, each containing sulfur, nitrogen, or oxygen heteroatoms within five-membered aromatic rings, to predict their absorption maxima (λ_{max}). Table S1 presents the calculated λ_{max} values of the photoswitches. Compounds **a**–**i** consist of a 5-membered heteroarene (R1) and a phenyl ring (R2) on either side of the azo bond (–N=N–), while compounds **j**–**x** are azoheteroarenes featuring either identical or different 5-membered heteroarenes (R1 and R2).

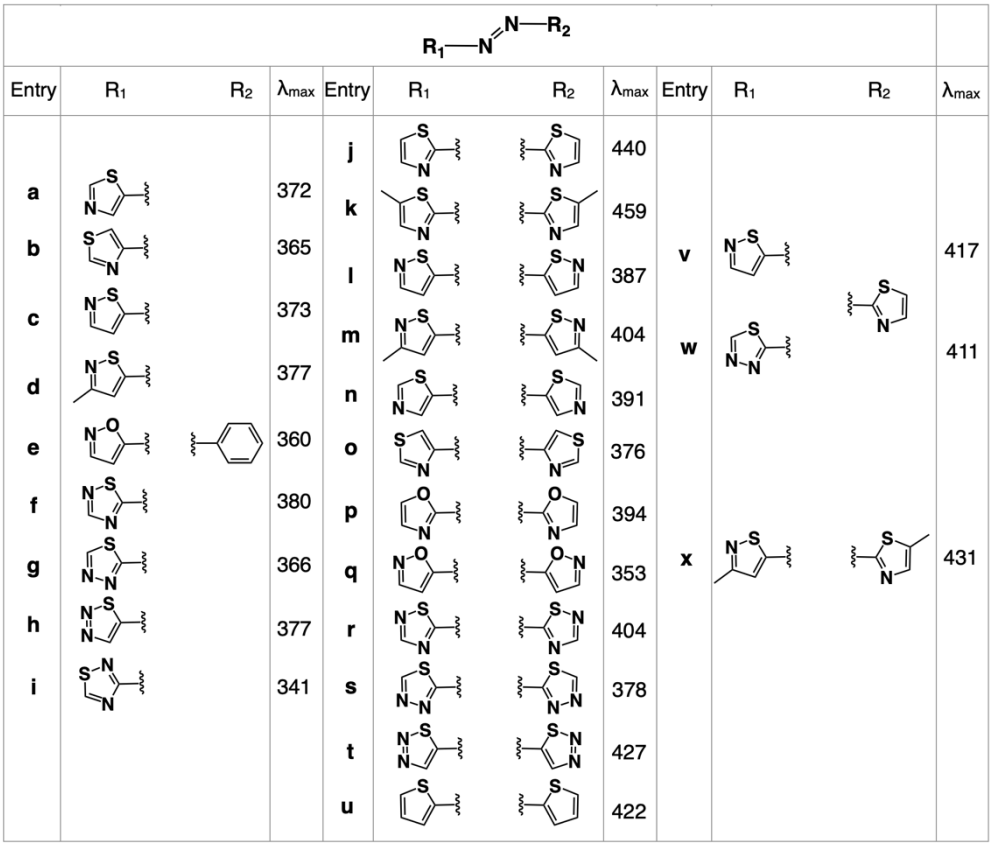

Table **S1**: Table showing the part of molecular structures of heteroaryl azophotoswitches designed along with their calculated λ_{max} values. R1 and R2 are phenyl or 5-membered heteroaryl units.

3. Synthesis

Synthesis of **photoswitches 1-3**

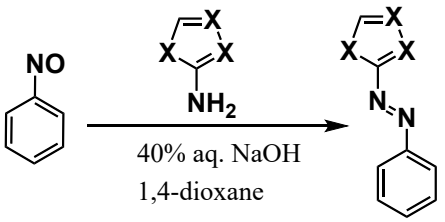

X = H, N or S

Scheme S1: Synthetic scheme for compounds **1-3**.

Compound **1**: To a warm (40 °C) NaOH solution (40% aq., 1 mL), 5-amino-3-methylisothiazole hydrochloride (2.3 mmol) in 1,4-dioxane (2.5 mL) was added and gently heated to 60 °C. Then, nitrosobenzene (2.53 mmol) was added slowly, and the mixture was stirred for 2 hours. The reaction mixture was then cooled and quenched with water and extracted with ethyl acetate (3 x 25 mL). The organic layer was washed with brine, dried over MgSO4, and concentrated *in vacuo*. The target compound was then isolated by column chromatography using a 2% ethyl acetate in hexane mixture, yielding an orange solid. (10.56%). ^{1}H NMR (400 MHz, $CDCl_3$) δ 7.89 (d, *J* = 9.6 Hz, 2H), 7.59 (s, 1H), 7.51 (m, 3H), 2.55 (s, 3H). ^{13}C NMR (400 MHz, $CDCl_3$) δ 179.3, 167.4, 151.9, 132.6, 129.4, 125.0, 123.5, 19.8.

Compound **2**: To a warm (40 °C) NaOH solution (40% aq., 1 mL), 2-amino-1,3,4-thiadiazole (2.3 mmol) in 1,4-dioxane (2.5 mL) was added and gently heated to 60 °C. Then, nitrosobenzene (2.53 mmol) was added slowly, and the mixture was stirred for 2 hours. The reaction mixture was then cooled and quenched with water and extracted with ethyl acetate (3 x 25 mL). The organic layer was washed with brine, dried with $MgSO_4$, and concentrated *in vacuo* followed by isolation of target compound by column chromatography using 20% ethyl acetate: hexane affording orange solid (14%). ^{1}H NMR (400 MHz, $CDCl_3$) δ 9.14 (s, 1H), 8.11 (d, *J* = 12.5 Hz, 2H), 7.62 - 7.56 (m, 3H). ^{13}C NMR (400 MHz, $CDCl_3$) δ 179.9, 153.0, 151.6, 134.3, 129.6, 124.4.

Compound **3**: To a warm (40 °C) NaOH solution (40% aq., 1 mL), 5-amino-1,2,3-thiadiazole (2.3 mmol) in 1,4-dioxane (2.5 mL) was added and gently heated to 60 °C. Then, nitrosobenzene (2.53 mmol) was added slowly, and the mixture was stirred for 2 hours. The reaction mixture was then cooled and quenched with water and extracted with ethyl acetate (3 x 25 mL). The organic layer was washed with brine, dried with $MgSO_4$, and concentrated *in vacuo* followed by isolation of target compound by column chromatography using 60% dichloromethane: hexane affording orange solid (4.0%). ^{1}H NMR (400 MHz, $CDCl_3$) δ 9.24 (s, 1H), 7.95 (d, *J* = 12.3 Hz, 2H), 7.58 - 7.53 (m, 3H). ^{13}C-NMR (400 MHz, $CDCl_3$) δ 171.0, 152.1, 146.6, 133.7, 129.5, 123.8.

Synthesis of **photoswitches 4-8**

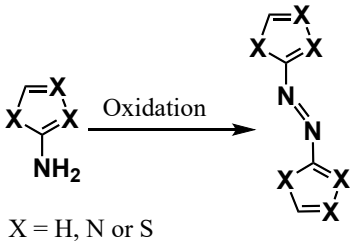

X = H, N or S

Scheme S2: Synthetic scheme for compounds **4**-**8**.

Compound **4**: To cold sodium hypochlorite solution (15 mL), cool suspension of 5-amino-1,2,4-thiadiazole (2.9 mmol) in dichloromethane (10 mL) was added little by little followed by stirring for 1 hour at 0 ˚C. The reaction mixture was quenched with water and extracted with dichloromethane (3 x 25 mL). The organic layer was washed with brine, dried over MgSO4, and concentrated *in vacuo*. The target compound was isolated by column chromatography using ethyl acetate: hexane (10:90, v/v) as the eluent, yielding an orange solid (36.0%). ^{1}H NMR (400 MHz, $CDCl_3$) δ 8.96 (s, 2H). ^{13}C-NMR (400 MHz, $CDCl_3$) δ 192.2, 164.1.

Compound **5**: 5-amino-1,2,3-thiadiazole (5 mmol) was dissolved in dichloromethane (50 mL). Potassium permanganate (15 mmol) and ferrous sulfate heptahydrate (10 mmol) were ground together until homogenous. The resulting powder was added to the dichloromethane solution. The mixture was stirred for 24 hours at room temperature. Afterward, the reaction mixture was filtered through celite, and the solvent evaporated. Finally, the target compound was isolated using column chromatography by 15% ethyl acetate: hexane affording orange red solid (4.6%). ^{1}H NMR (400 MHz, $CDCl_3$) δ 9.29 (s, 2H). ^{13}C-NMR (400 MHz, $CDCl_3$) δ 168.8, 148.5.

Compound **6**: 2-amino-5-methylthiazole (4.38 mmol) was dissolved in dichloromethane (50 mL). Potassium permanganate (13.2 mmol) and ferrous sulfate heptahydrate (8.76 mmol) were ground together until homogenous. The resulting powder was added to the dichloromethane solution. The mixture was stirred for 24 hours at room temperature. Afterward, the reaction mixture was filtered through celite, and the solvent evaporated. Finally, the compound was isolated by column chromatography by 30% ethyl acetate: hexane affording orange red solid (18.3%). ^{1}H NMR (400 MHz, $CDCl_3$) δ 7.78 (s, 1H), 2.56 (s, 3H). ^{13}C NMR (400 MHz, $CDCl_3$) δ 173.3, 143.4, 139.9, 13.2.

Compound **7**: 5-amino-3-methylisothiazole hydrochloride (3.3 mmol) was dissolved in dichloromethane (50 mL). Potassium permanganate (6.6 mmol) and ferrous sulfate heptahydrate (4.4 mmol) were ground together until homogenous. The resulting powder was added to the dichloromethane solution. The mixture was stirred for 24 hours at room temperature. Afterward, the reaction mixture was filtered through celite, and the solvent evaporated. Finally, the target compound was isolated using column chromatography by 2% ethyl acetate: hexane affording orange solid (35.5%). ^{1}H NMR (400 MHz, $CDCl_3$) δ 7.58 (s,

1H), 2.54 (s, 3H). ^{13}C NMR (400 MHz, $CDCl_3$) δ 177.7, 167.7, 126.5, 19.7.

Compound **8**: 2-amino-5-methylthiazole (8.75 mmol) and 5-amino-3-methylisothiazole hydrochloride (8.75 mmol) was dissolved in dichloromethane. Potassium permanganate (26.25 mmol) and ferrous sulfate heptahydrate (17.5 mmol) were ground together until homogenous. The resulting powder was added to the dichloromethane solution. The mixture was stirred for 24 hours at room temperature. Afterward, the reaction mixture was filtered through celite, and the solvent evaporated. Finally, the target compound was isolated using column chromatography by 10% ethyl acetate: hexane affording orange red solid (7.3%). ^{1}H NMR (400 MHz, $CDCl_3$) δ 7.77 (s, 1H), 7.61 (s, 1H), 2.57 (s, 3H), 2.55 (s, 3H). ^{13}C NMR (400 MHz, $CDCl_3$) δ 177.5, 173.4, 167.4, 143.4, 139.8, 126.1, 19.7, 13.1.

4. NMR spectra (^{1}H, ^{13}C) and Mass spectra of compounds 1-8.

Compound **1**

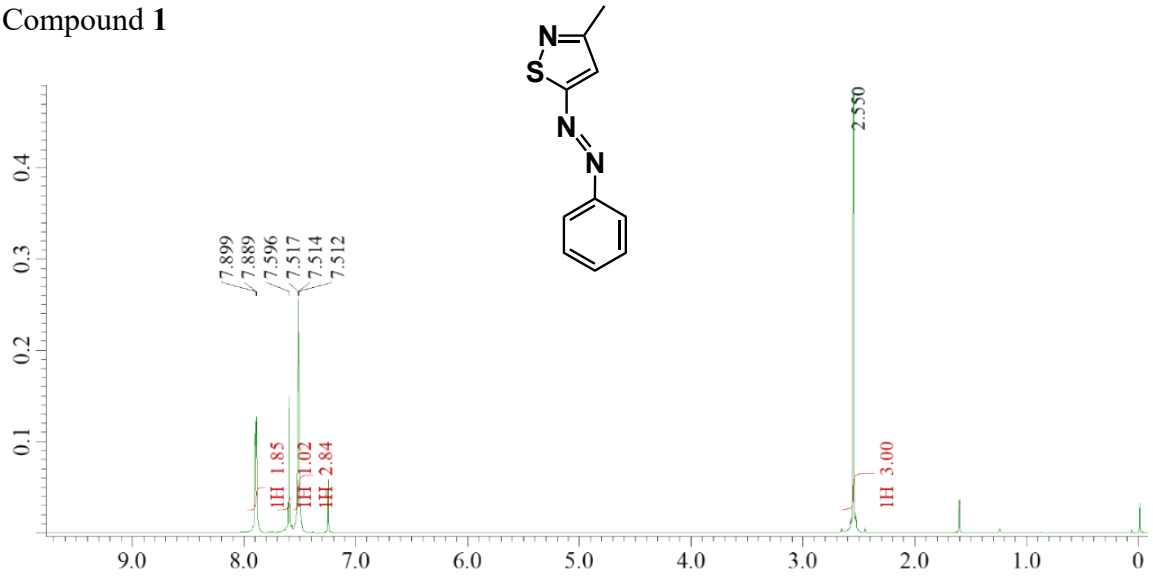

Figure S1: ^{1}H NMR of compound **1** in $CDCl_3$.

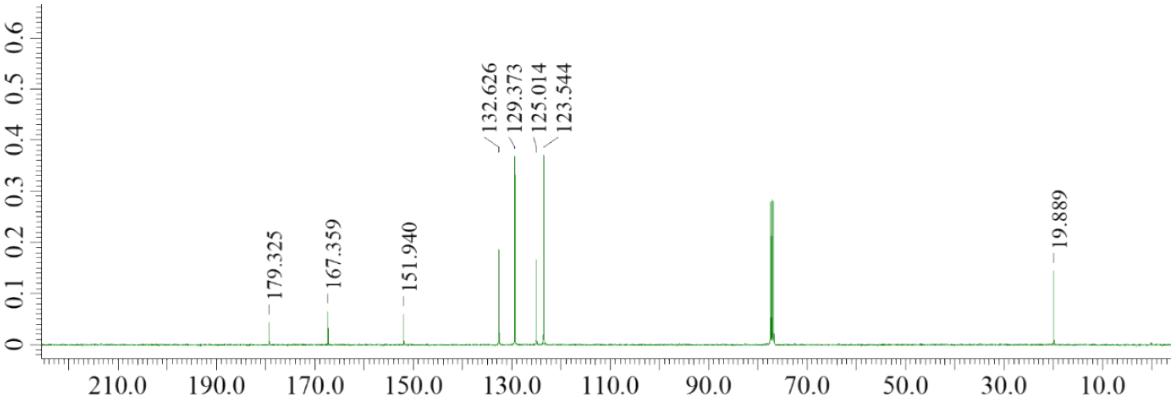

Figure S2: ^{13}C NMR of compound **1** in $CDCl_3$.

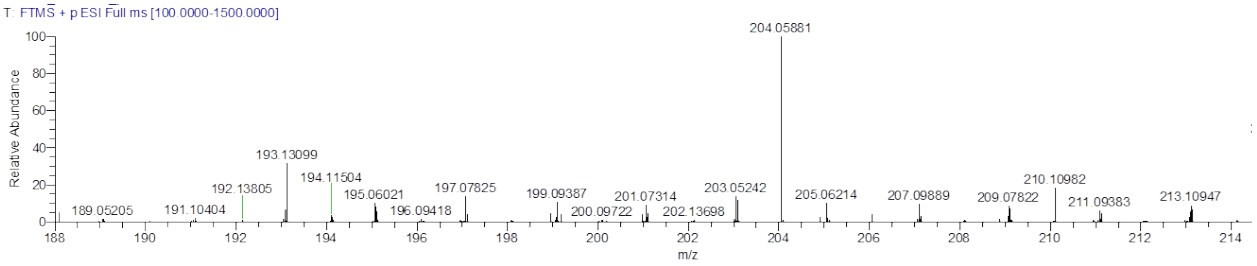

Figure S3: High-resolution mass spectra (ESI) of compound **1**. *m/z* $[M + H]^+$ calculated for $C_{10}H_9N_3S$: 204.0595, found: 204.0588

Compound **2**

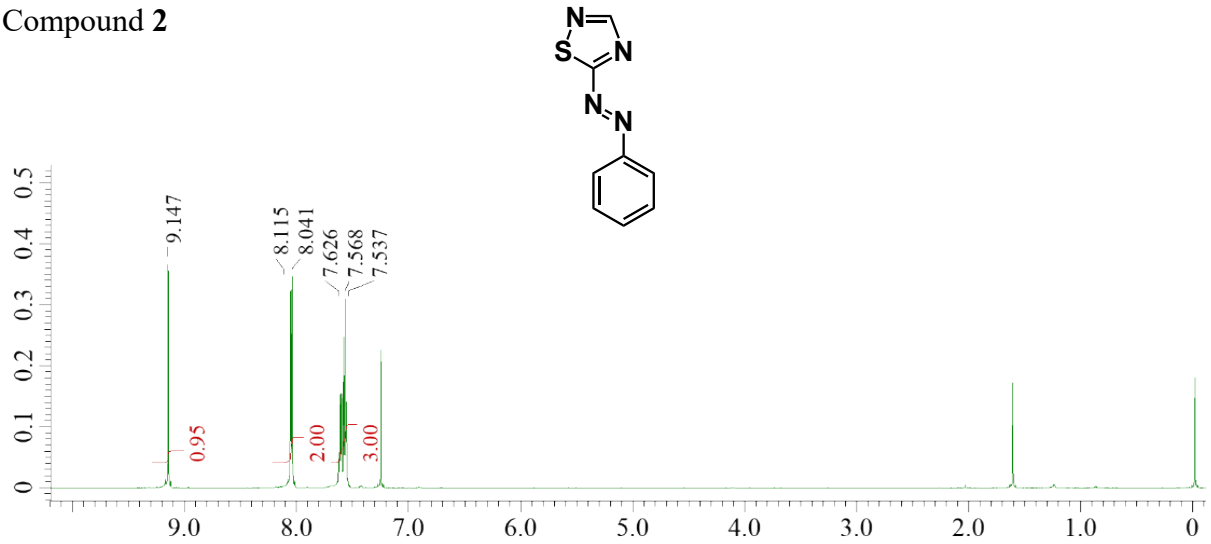

Figure S4: ^{1}H NMR of compound **2** in $CDCl_3$.

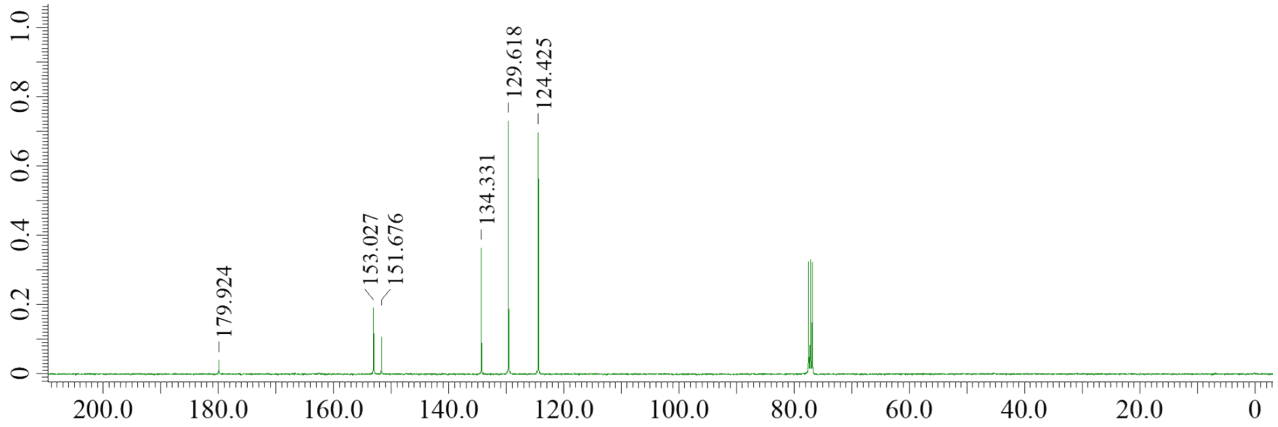

Figure S5: ^{13}C NMR of compound **2** in $CDCl_3$.

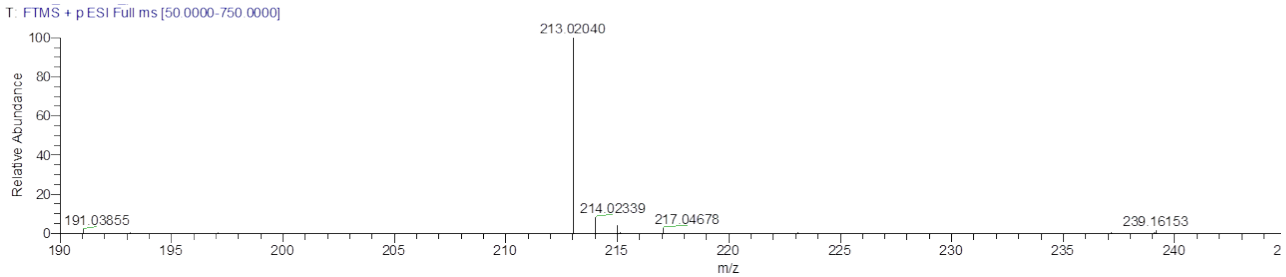

Figure S6: High-resolution mass spectra (ESI) of compound **2.** *m/z* $[M + Na]^+$ calculated for $C_8H_6N_4S$: 213.0211, found: 213.0204.

Compound **3**

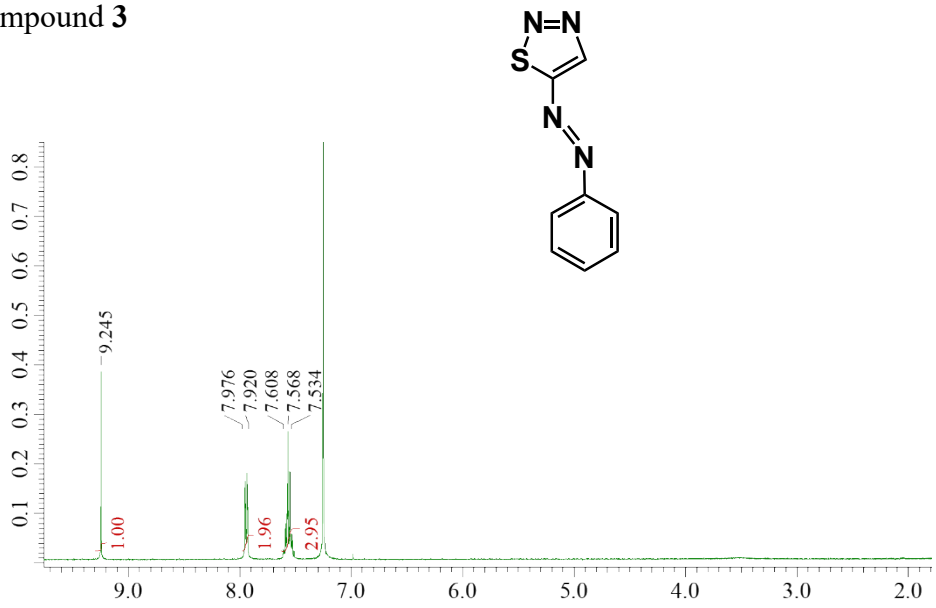

Figure S7: ^{1}H NMR of compound **3** in $CDCl_3$.

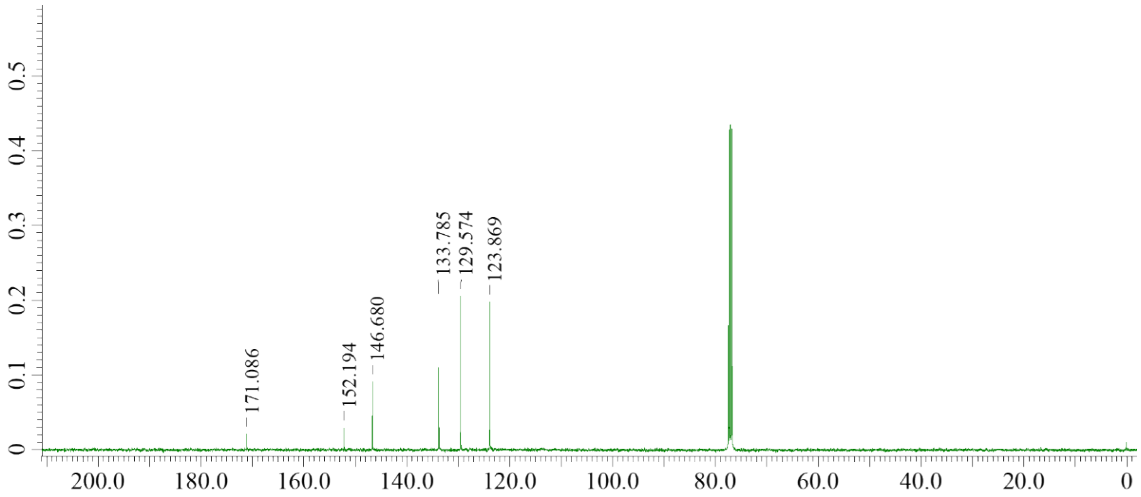

Figure S8: ^{13}C NMR of compound **3** in $CDCl_3$.

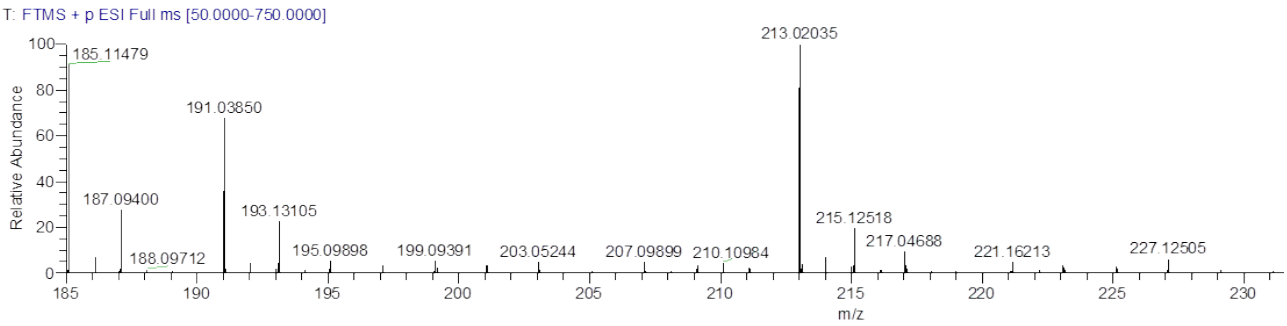

Figure S9: High-resolution mass spectra (ESI) of compound **3.** *m/z* $[M + Na]^+$ calculated for $C_8H_6N_4S$: 213.0211, found: 213.0203.

Compound **4**

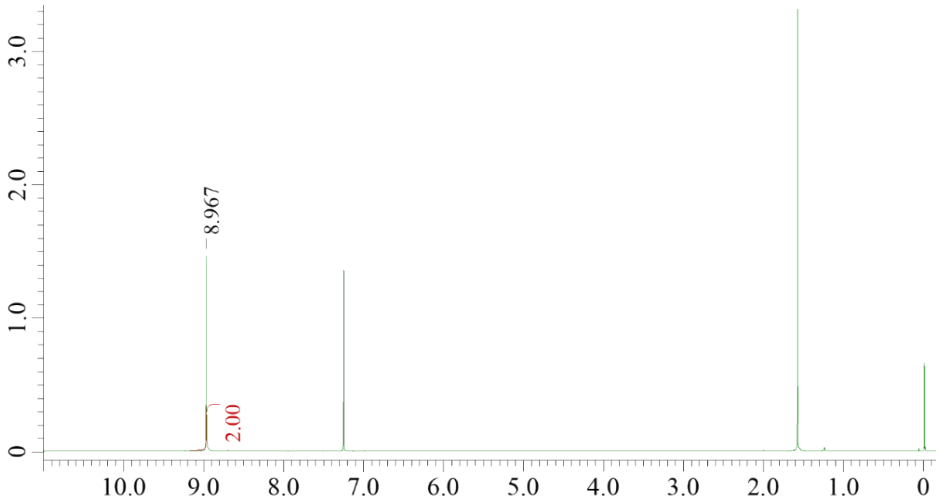

Figure S10: ^{1}H NMR of compound **4** in $CDCl_3$.

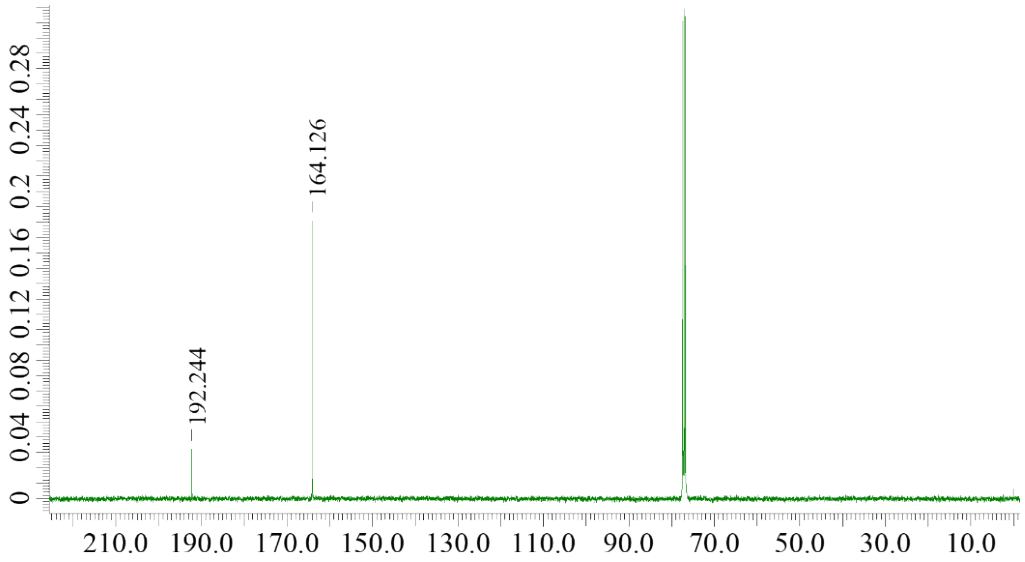

Figure S11: ^{13}C NMR of compound **4** in $CDCl_3$.

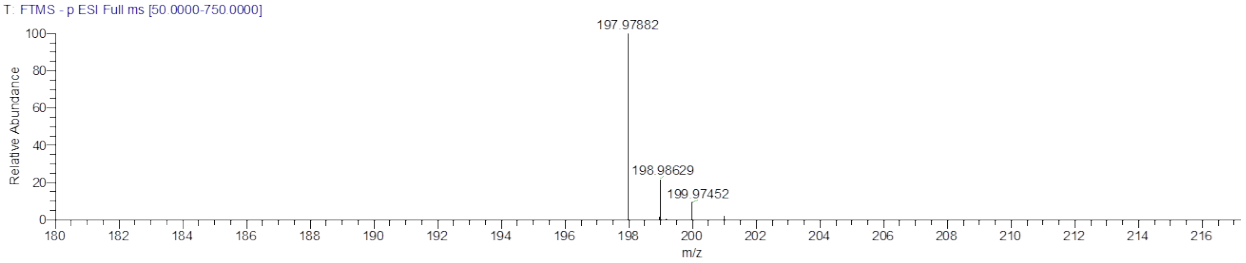

Figure S12: High-resolution mass spectra (ESI) of compound **4.** *m/z* $[M]^+$ calculated for $C_4H_2N_6S_2$: 197.9782, found: 197.9788.

Compound **5**

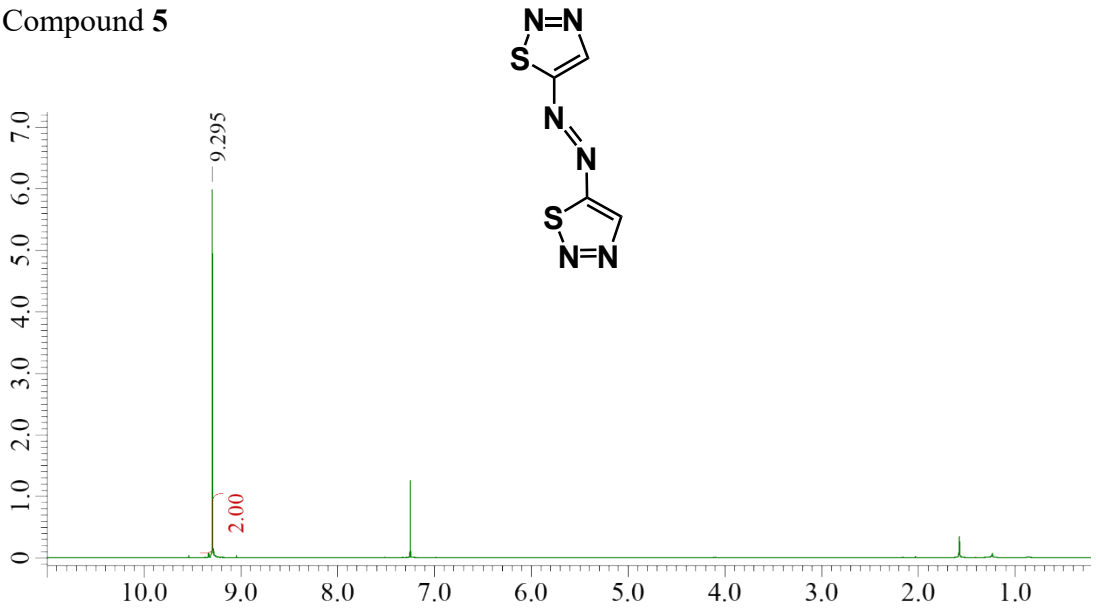

Figure S13: ^{1}H NMR of compound **5** in $CDCl_3$.

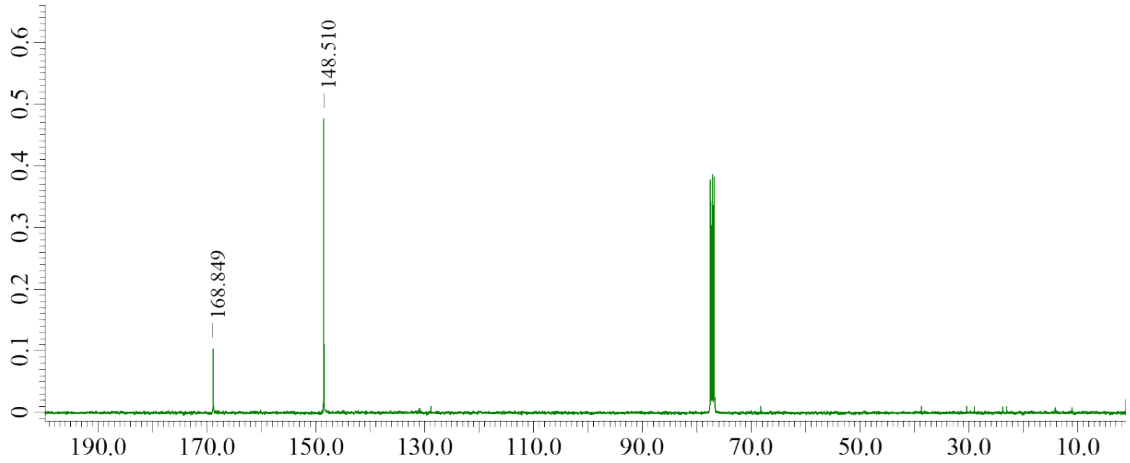

Figure S14: ^{13}C NMR of compound **5** in $CDCl_3$.

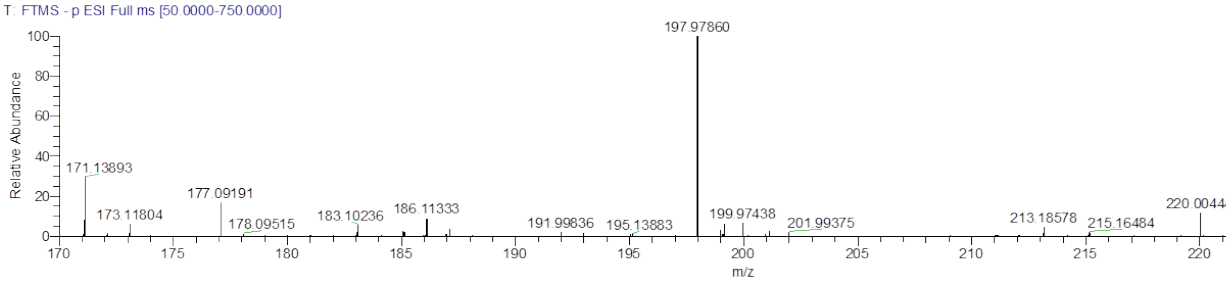

Figure S15: High-resolution mass spectra (ESI) of compound **5.** *m/z* $[M]^+$ calculated for $C_4H_2N_6S_2$: 197.9782, found: 197.9786.

Compound **6**

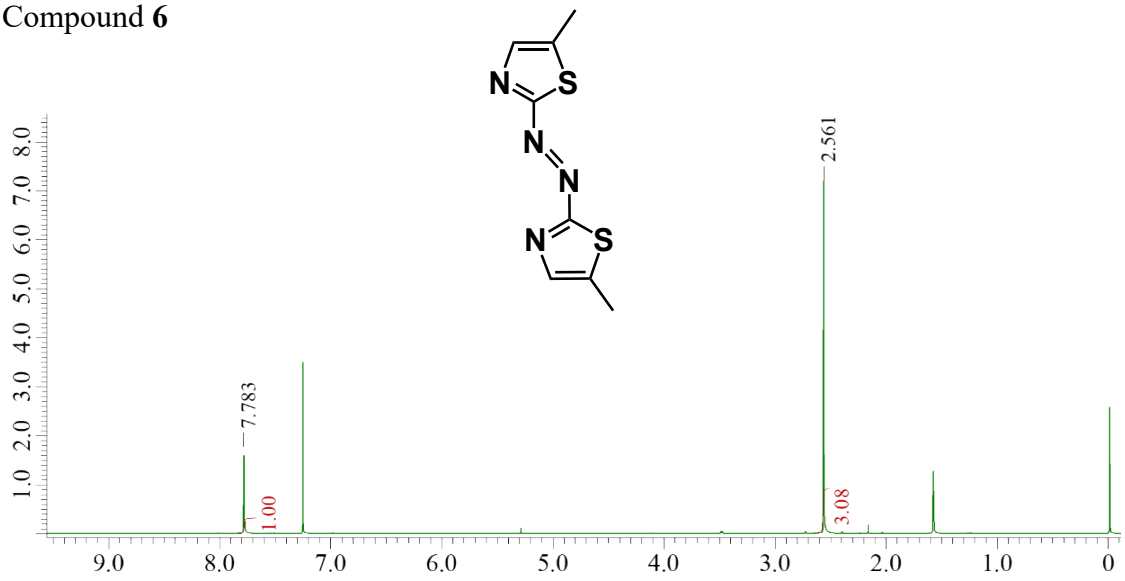

Figure S16: ^{1}H NMR of compound **6** in $CDCl_3$.

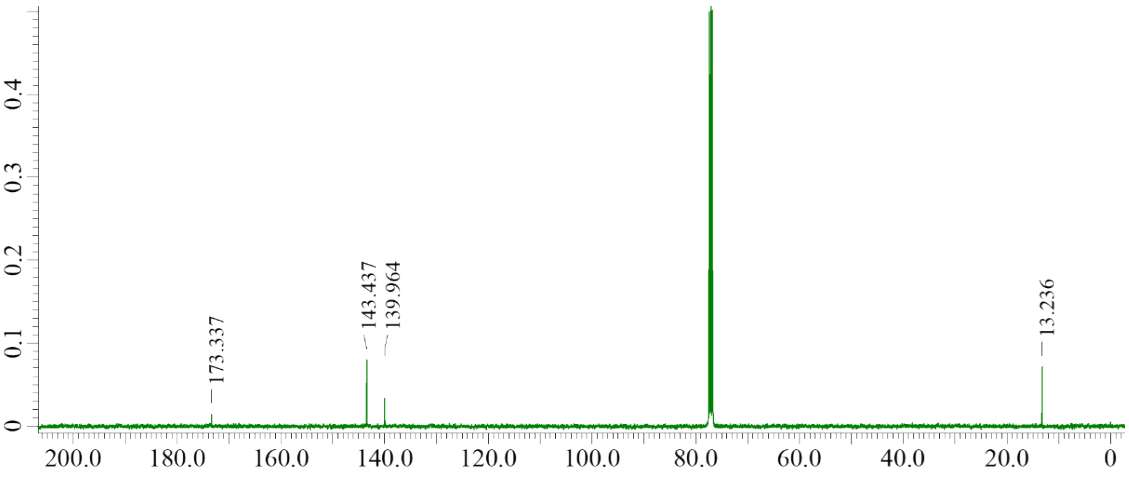

Figure S17: ^{13}C NMR of compound **6** in $CDCl_3$.

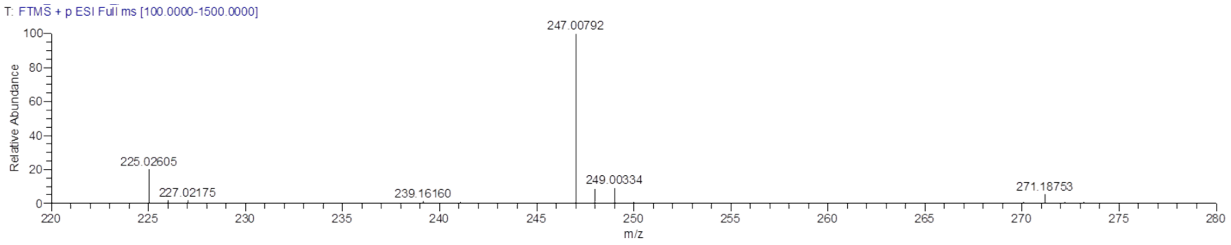

Figure S18: High-resolution mass spectra (ESI) of compound **6.** *m/z* $[M + Na]^+$ calculated for $C_8H_8N_4S_2$: 247.0088, found: 247.0079.

Compound **7**

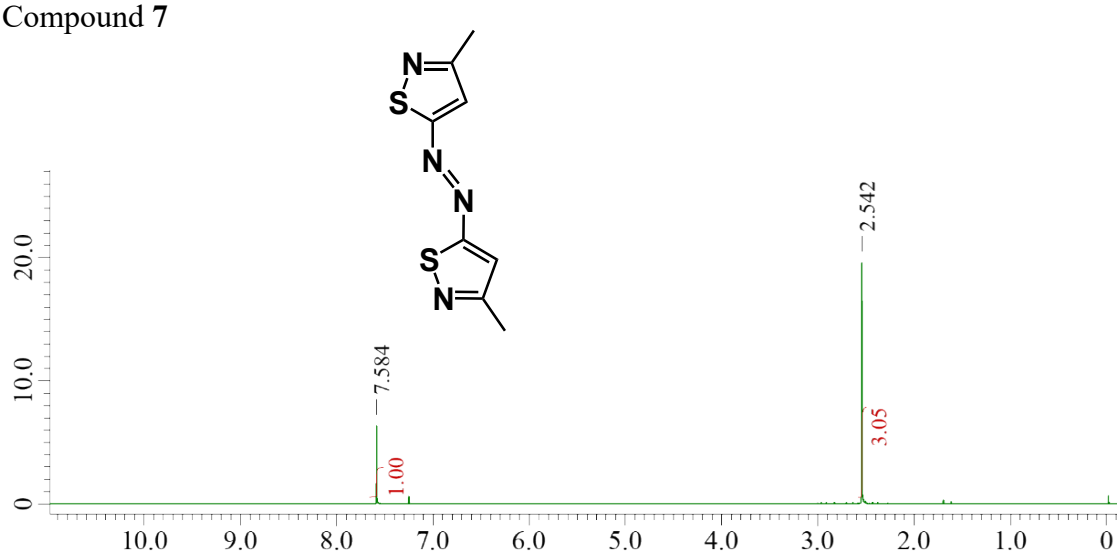

Figure S19: ^{1}H NMR of compound **7** in $CDCl_3$.

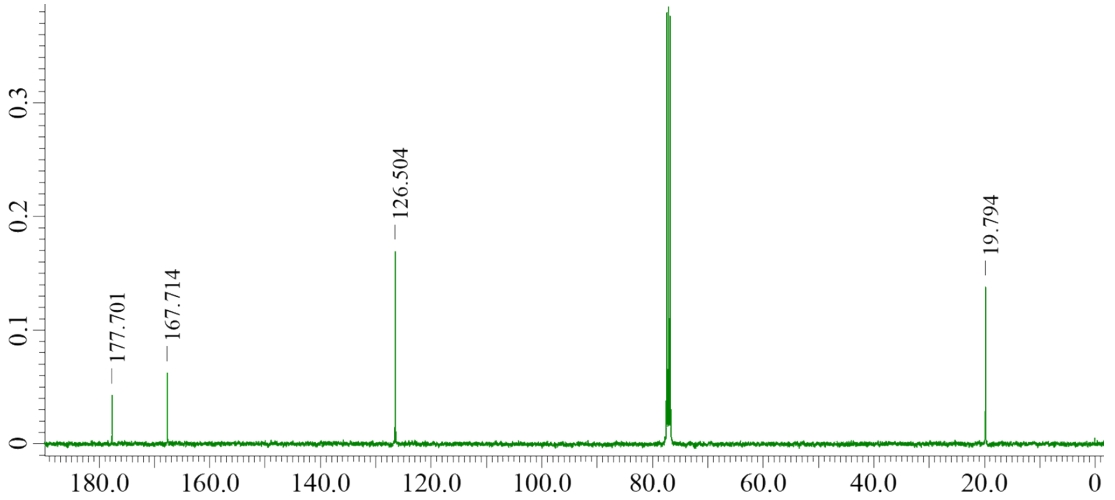

Figure S20: ^{13}C NMR of compound **7** in $CDCl_3$.

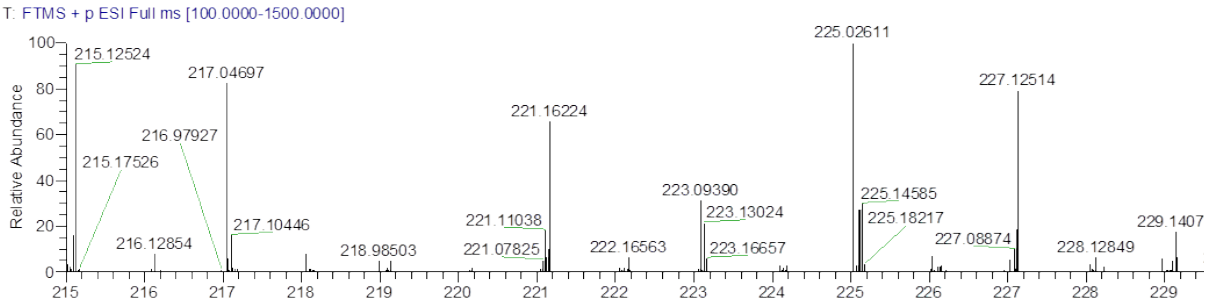

Figure S21: High-resolution mass spectra (ESI) of compound **7.** *m/z* $[M + H]^+$ calculated for $C_8H_8N_4S_2$: 225.0269, found: 225.0261, 227.1251.

Compound **8**

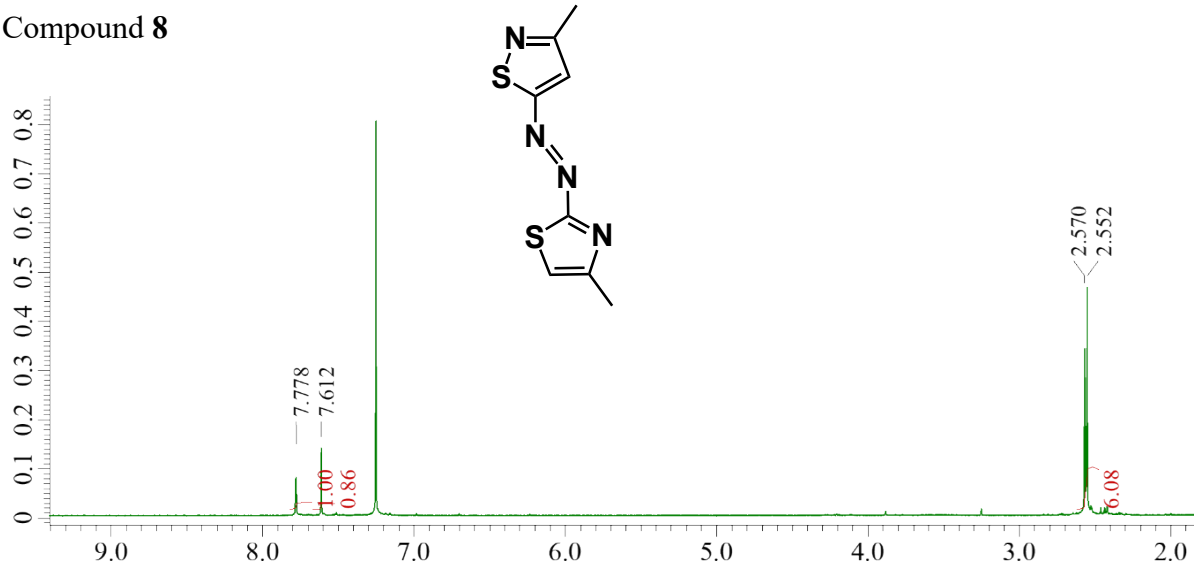

Figure S22: ^{1}H NMR of compound **8** in $CDCl_3$.

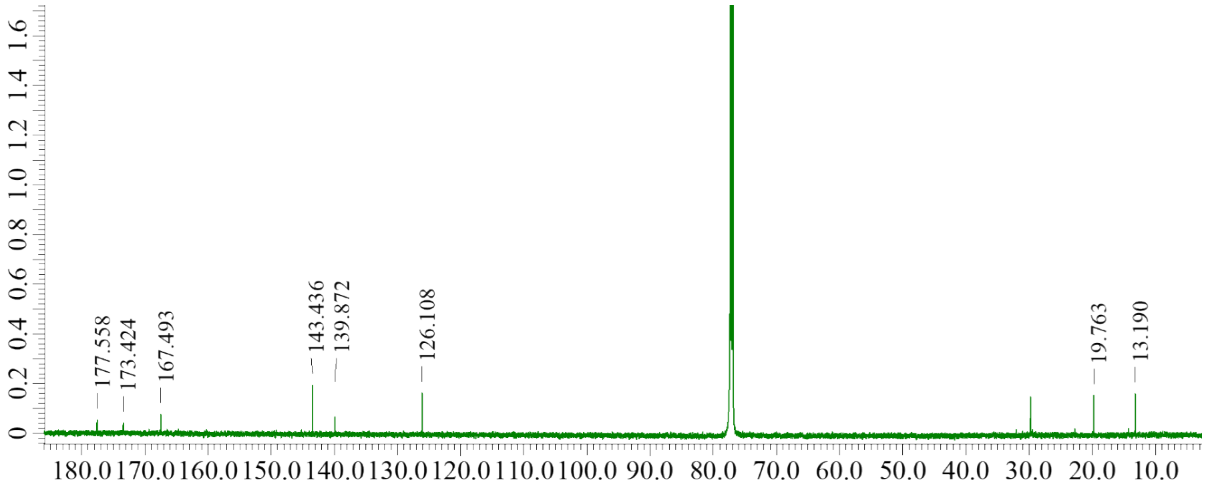

Figure S23: ^{13}C NMR of compound **8** in $CDCl_3$.

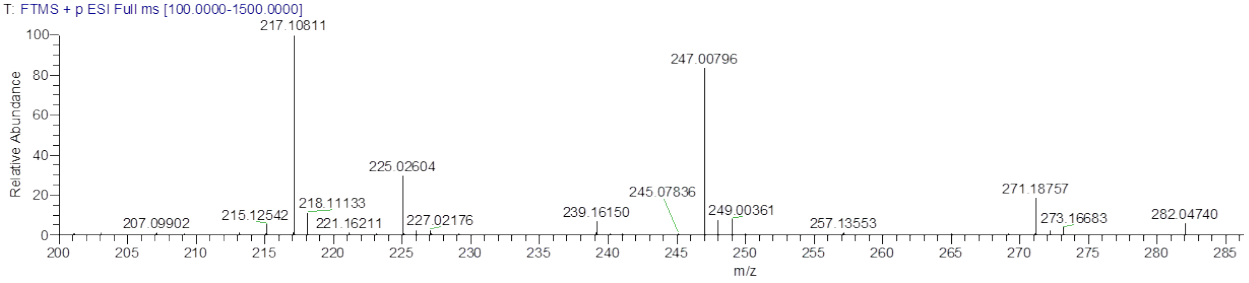

Figure S24: High-resolution mass spectra (ESI) of compound **8.** *m/z* $[M + Na]^+$ calculated for

$C_8H_8N_4S_2$: 247.0088, found: 247.0079.

5. Absorption spectra (Zoom-in 400 nm–650 nm).

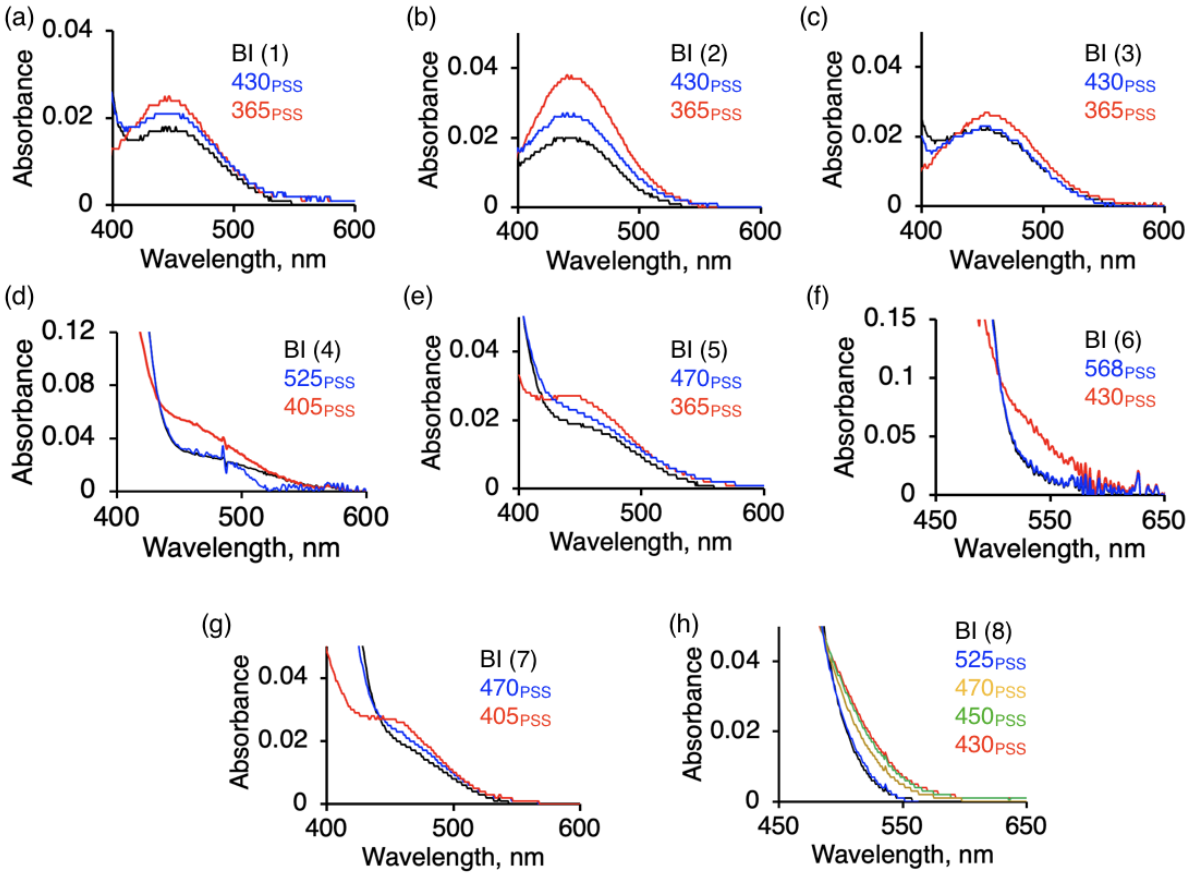

Figure S25: (a–h) UV−visible absorption spectra (Zoom-in) of **1**−**8** in acetonitrile at 25 °C before irradiation (BI, black lines) and at the *cis*-rich PSS under 365, 405 or 430 nm irradiations (365_{PSS}, 405_{PSS}, 430_{PSS}; red lines) and at *trans*-rich PSS under 430, 470, 525 or 568 nm irradiations (430_{pss}, 470_{PSS}, 525_{PSS}, 568_{PSS}; blue lines). In (h), intermediate PSSs under 450 and 470 nm are added (450_{PSS} and 470_{PSS}; green and yellow lines, respectively). In (d), the 525_{PSS} curve shows a decrease in absorbance beyond 500 nm, attributed to the effect of continuous irradiation by 525 nm light during spectral recording.

6. Thermal back isomerization

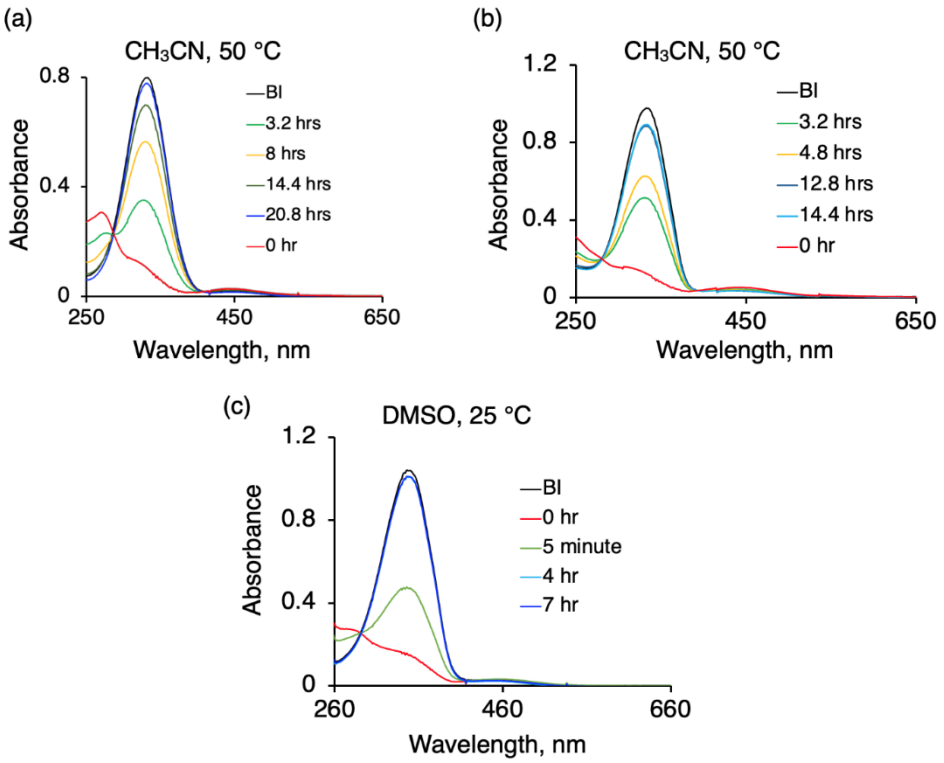

Figure S26: (a-c) UV-visible absorption Spectra are shown before irradiation (BI), at the *cis*-rich photostationary state under 365 nm irradiation (365_{PSS}, 0 hr), and at the *trans*-rich state after thermal relaxation. (a) for compound **1** in acetonitrile at 50 °C 20.8 hours, (b) for compound **2** in acetonitrile at 50 °C for 14.4 hours and (c) for compound **3** in DMSO at 25 °C for 7 hours.

7. Measurement of isomer conversion at PSS.

A.) Isomer conversion measurement at PSS by NMR (compound 1,2,3 and 7).

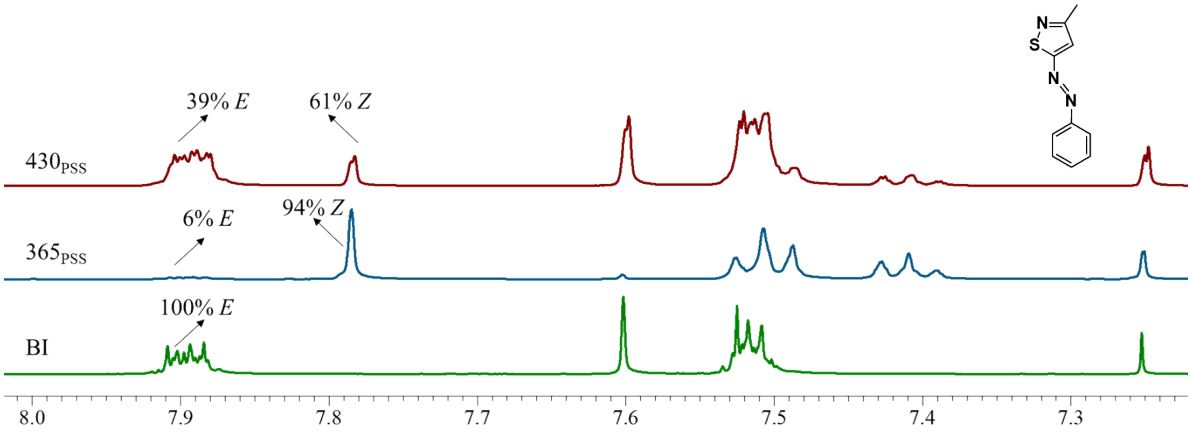

Figure S27: ^{1}H NMR spectra (400 MHz, $CDCl_3$) of compound **1** obtained before irradiation (BI) and irradiations at PSS of 365 nm (365_{PSS}) and 525 nm (430_{PSS}) at 25 °C.

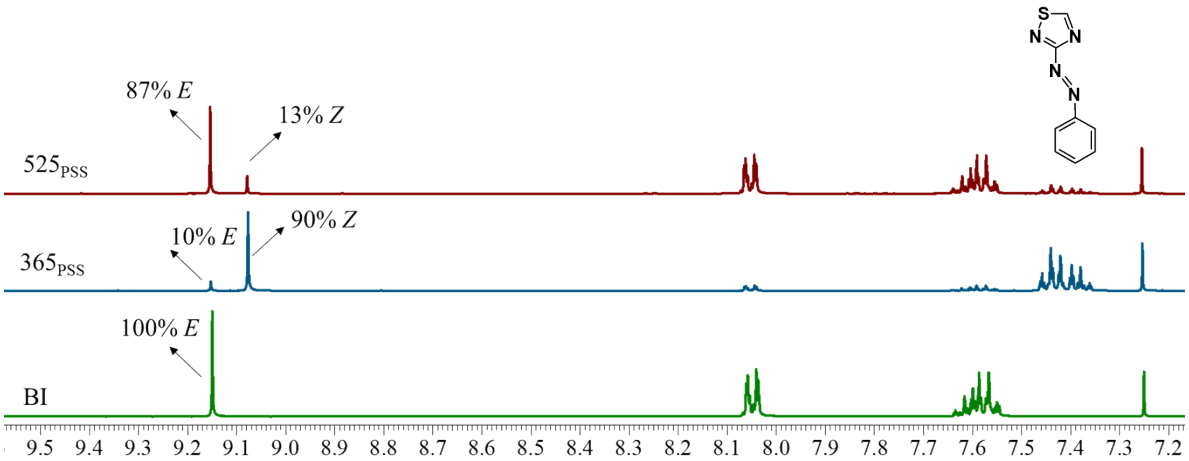

Figure S28: ^{1}H NMR spectra (400 MHz, $CDCl_3$) of compound **2** obtained before irradiation (BI) and irradiations at PSS of 365 nm (365_{PSS}) and 525 nm (525_{PSS}) at 25 °C.

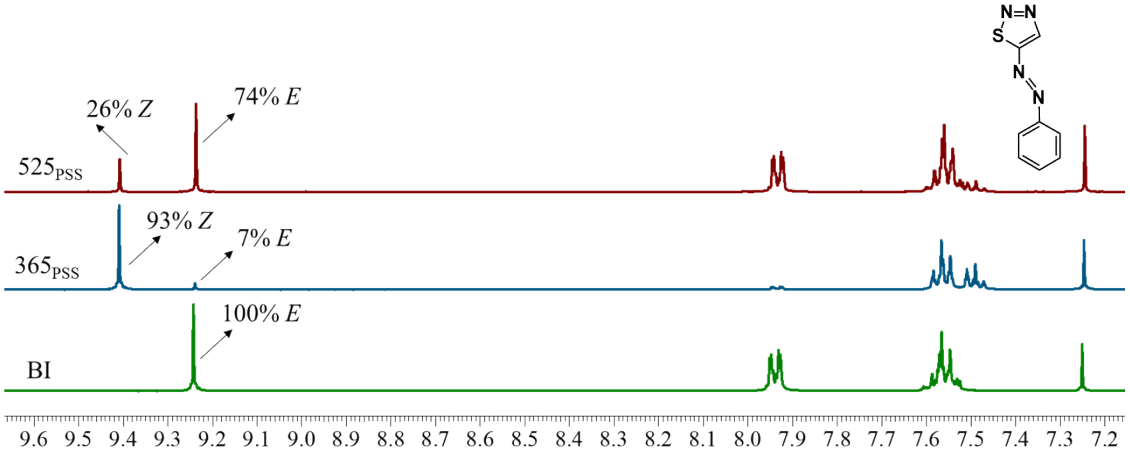

Fig ure

S29: ^{1}H NMR spectra (400 MHz, $CDCl_3$) of compound **3** obtained before irradiation (BI) and irradiations at PSS of 365 nm (365_{PSS}) and 525 nm (525_{PSS}) at 25 °C.

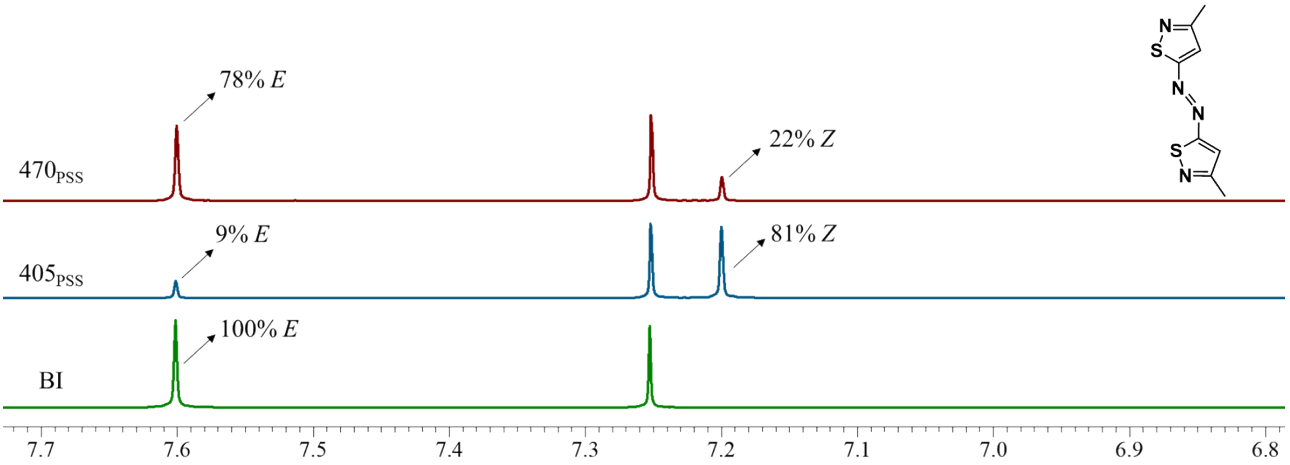

Figure S30: ^{1}H NMR spectra (400 MHz, $CDCl_3$) of compound **7** obtained before irradiation (BI) and irradiations at PSS of 405 nm (405_{PSS}) and 470 nm (470_{PSS}) at 25 °C.

B.) Isomer conversion measurement at PSS by absorption spectra (compound 4,5,6 and 8)

Because of the short half-lives of compounds **4**,**5**,**6** and **8**, NMR analysis was not feasible for determining the isomer ratios at PSS. Therefore, absorption spectroscopy was used to calculate the isomer ratios at PSS. When the extinction coefficient of the Z isomer of the photoswitch (ε_Z) at λ_{max} was greater than zero, the minimum conversion (%) from *E* to *Z* at PSS were calculated as $\frac{A_0 - A_{PSS}}{A_0} \times 100$ using the following equation:

$$Conversion\ (\%) from\ E\ to\ Z \quad = \frac{A_{PSS} - A_{PSS,\ E}}{A_0} \times 100 = \frac{A_0 - (A_{PSS} - A_{PSS,\ Z})}{A_0} \times 100$$

$$> \frac{A_0 - A_{PSS}}{A_0} \times 100$$

A_0 Absorbance at initial state (100% *trans*) at λ_{max}

A_{PSS} Absorbance at PSS at λ_{max}

$A_{PSS,\ E}$ A portion of absorbance at PSS at λ_{max}, contributed by *E* isomer

$A_{PSS,\ Z}$ A portion of absorbance at PSS at λ_{max}, contributed by *Z* isomer

8. Measurement of half-life

For a first order reaction, half-life ($t_{1/2}$) can be calculated using the equation:

$$t_{1/2} = 0.693/k$$

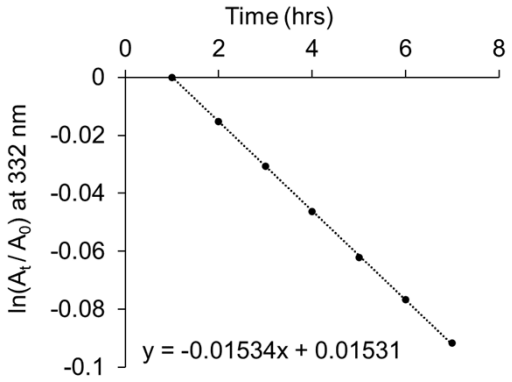

Figure S31: Graph showing the linear fit of the change in absorbance at 332 nm over time at 25 °C for compound **1.** Rate constant k (= slope) is mentioned, $t_{½}$ = 45.2 hours.

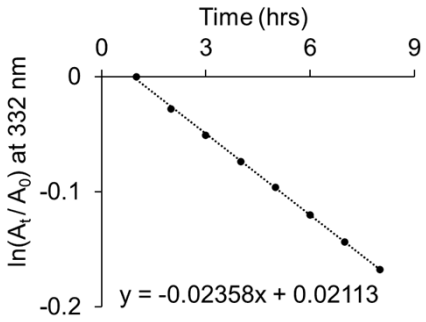

Figure S32: Graph showing the linear fit of the change in absorbance at 332 nm over time at 25 °C for compound **2.** Rate constant k (= slope) is mentioned, $t_{½}$ = 29.4 hours.

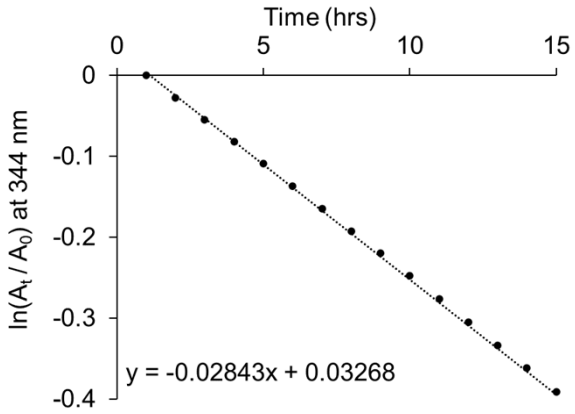

Figure S33: Graph showing the linear fit of the change in absorbance at 344 nm over time at 25 °C for compound **3.** Rate constant k (= slope) is mentioned, $t_{½}$ = 24.3 hours.

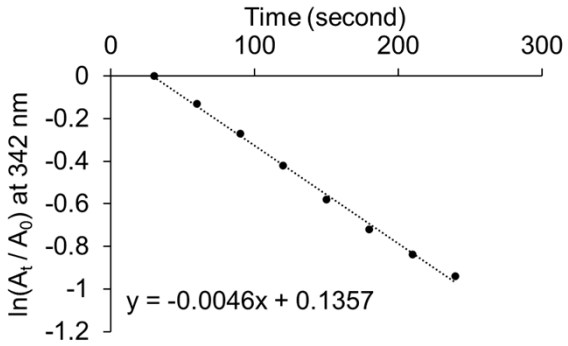

Figure S34: Graph showing the linear fit of the change in absorbance at 342 nm over time at 25 °C for compound **5.** Rate constant *k* (= slope) is mentioned, $t_{½}$ = 3 minutes.

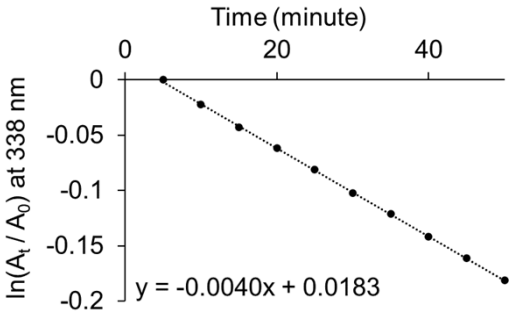

Figure S35: Graph showing the linear fit of the change in absorbance at 338 nm over time at 25 °C for compound **7.** Rate constant *k* (= slope) is mentioned, $t_{½}$ = 2.9 hours.

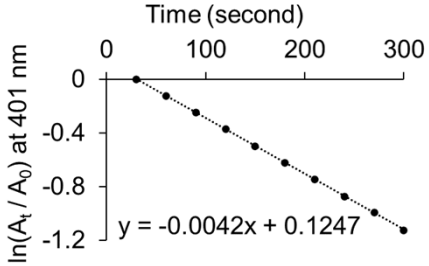

Figure S36: Graph showing the linear fit of the change in absorbance at 338 nm over time at 25 °C for compound **8.** Rate constant *k* (= slope) is mentioned, $t_{½}$ = 2.7 minutes.

9. Single crystal X-ray structure analysis [1-3]

CCDC 2371070 for **2** (*trans*), 2371071 for **2** (*cis*), 2371069 for **3** (*trans*), 2371067 for **3** (*cis*), 2371065 for **4,** 2371066 for **5,** 2371068 for **6,** 2371072 for **8** contain the supplementary crystallographic data for this paper.

10. Time-dependent density-functional theory (TDDFT) calculations [4-10]

Table S2. Cartesian coordinates of ground state optimized geometry of **a**.

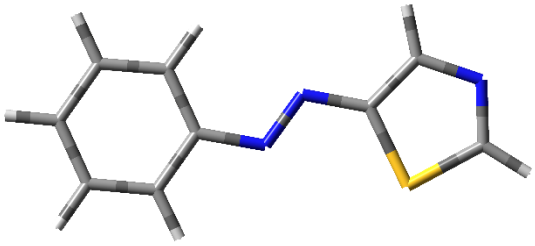

	X	Y	Z
S	2.554615	-1.18844	-5.9E-05
N	-0.3112	-0.37116	0.000087
N	0.432275	0.652256	-4E-06
C	-1.70246	-0.12225	0.000042
C	-2.29075	1.158604	-0.0001
H	-1.65894	2.039248	-0.00018
C	1.784937	0.401652	-1.7E-05
C	-2.51435	-1.26845	0.000152
H	-2.04023	-2.24505	0.00026
C	-4.48826	0.12855	-0.00002
H	-5.56927	0.230367	-4.4E-05
C	-3.6775	1.274684	-0.00013
H	-4.1343	2.259826	-0.00024
C	-3.90439	-1.14201	0.000121
H	-4.52847	-2.03018	0.000207
C	4.089457	-0.36731	0.000278
H	5.010867	-0.93845	0.000331
C	2.753899	1.383782	-0.00016
N	4.051476	0.943388	-0.0001
H	2.535116	2.444355	-0.00027

Table S3. Cartesian coordinates of ground state optimized geometry of **b**.

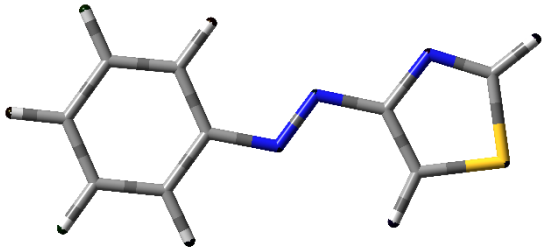

	X	Y	Z
N	-0.43435	-0.43417	0.000029
N	0.315021	0.57959	-3.6E-05
C	-1.82525	-0.16795	0.000046
C	-2.39895	1.119084	-2E-06
H	-1.75639	1.991863	-5.7E-05
C	-2.64976	-1.3044	0.000117
H	-2.18634	-2.28616	0.000154
C	-4.60805	0.11402	0.000093
H	-5.68787	0.22812	0.000111
C	-3.78432	1.251019	0.000022
H	-4.23015	2.241217	-1.5E-05
C	-4.03876	-1.16287	0.000141
H	-4.67272	-2.04405	0.000196
C	1.690047	0.292469	-4.5E-05
C	2.310173	-0.94041	0.000058
N	2.538712	1.383404	-0.00014
S	4.016505	-0.73648	-0.00012
C	3.781398	0.998128	-1.8E-05
H	4.630408	1.670823	-6.8E-05
H	1.844191	-1.91455	0.00015

Table S4. Cartesian coordinates of ground state optimized geometry of **c**.

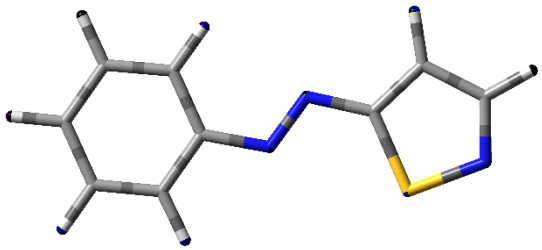

	X	Y	Z
S	-2.52244	-1.15989	-0.00065
N	0.304797	-0.32542	0
N	-0.42673	0.706157	0.000119
C	1.696832	-0.10061	0.000046
C	2.305625	1.171334	0.000226
H	1.688179	2.062024	0.000342
C	-1.78596	0.434333	0.000039
C	2.487596	-1.2621	-0.0001
H	1.995474	-2.22962	-0.00024
C	4.483227	0.101516	0.000106
H	5.565789	0.184887	0.000131
C	3.69337	1.262823	0.000252
H	4.168318	2.239182	0.00039
C	3.879127	-1.15955	-0.00007
H	4.488619	-2.05758	-0.00018
C	-2.77716	1.393175	-7.6E-05
H	-2.58978	2.45914	-0.00011
C	-4.05856	0.779118	0.000271
H	-4.99987	1.319906	0.000566
N	-4.09268	-0.54358	0.000642

Table S5. Cartesian coordinates of ground state optimized geometry of **d**.

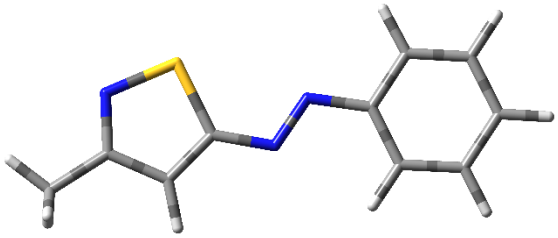

	X	Y	Z
S	-2.01475	-1.4323	0.000097
N	0.752877	-0.40602	-9.9E-05
N	-0.04842	0.572155	-0.00017
C	2.126221	-0.08279	-3.5E-05
C	2.642099	1.229345	0.000089
H	1.961756	2.072971	0.000144
C	-1.38626	0.208217	-8.4E-05
C	2.99856	-1.18414	-9.1E-05
H	2.577706	-2.18473	-0.00018
C	4.891219	0.319709	0.000078
H	5.964974	0.480708	0.000123
C	4.019709	1.420902	0.000146
H	4.4229	2.429011	0.000247
C	4.379249	-0.98145	-4.3E-05
H	5.051661	-1.83344	-9.5E-05
C	-2.43704	1.096151	-0.00019
H	-2.31677	2.172201	-0.00036
C	-3.69083	0.409739	-4.7E-05
N	-3.62296	-0.91342	0.000091
C	-5.02661	1.094845	0.000072
H	-5.13122	1.733314	0.88393
H	-5.13031	1.735548	-0.88225
H	-5.83319	0.359047	-0.0012

Table S6. Cartesian coordinates of ground state optimized geometry of **e**.

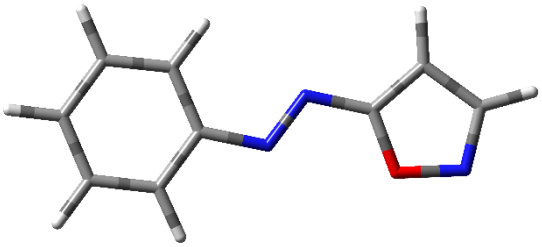

	X	Y	Z
N	0.044854	-0.44654	0.000084
N	-0.71982	0.562153	0.000118
C	-2.07197	0.273105	0.00004
O	-2.54906	-0.99853	-6.4E-05

C	-4.2633	0.330802	-1.9E-05
H	-5.30733	0.616194	-2.9E-05
N	-3.94986	-0.94848	-0.00012
C	-3.11545	1.162932	0.000051
H	-3.05724	2.239918	0.000121
C	1.425954	-0.16013	0.000031
C	2.265424	-1.28725	0.000051
C	1.980421	1.136708	-3.5E-05
C	3.651267	-1.12591	0.000013
H	1.814582	-2.27463	0.0001
C	3.362823	1.286971	-7.9E-05
H	1.325893	2.000472	-5.5E-05
C	4.200931	0.159805	-5.5E-05
H	4.298368	-1.99721	0.000033
H	3.7964	2.282334	-0.00013
H	5.278987	0.289005	-8.9E-05

Table S7. Cartesian coordinates of ground state optimized geometry of **f**.

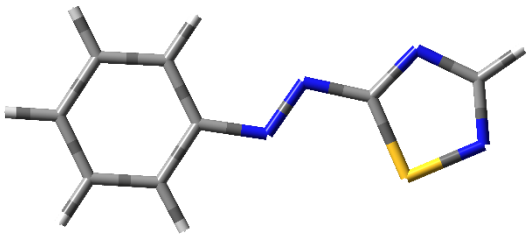

	X	Y	Z
S	2.508362	-1.15728	-1E-06
N	-0.28184	-0.28987	0.000055
N	0.441723	0.747213	0.000004
N	2.716265	1.396346	-0.00008
C	-1.67037	-0.08523	0.000032
C	-2.29487	1.180731	-0.00005
H	-1.68872	2.079063	-0.0001
C	1.802747	0.451984	-1.7E-05
C	-2.44341	-1.26022	0.000099
H	-1.9363	-2.21974	0.000162
C	3.950738	0.809411	-6.3E-05
H	4.843428	1.424903	-0.0001
C	-4.45421	0.077535	0.000006
H	-5.53775	0.146196	-5E-06
C	-3.68225	1.251936	-6.3E-05
H	-4.17254	2.220377	-0.00013
C	-3.83518	-1.17649	0.000087
H	-4.43364	-2.08159	0.00014
N	4.059931	-0.5038	0.000002

Table S8. Cartesian coordinates of ground state optimized geometry of **g**.

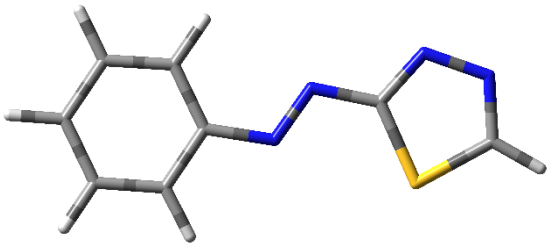

	X	Y	Z
S	2.522988	-1.1818	0.000097
N	-0.28442	-0.32098	0.000044
N	0.4454	0.709525	-0.00002
N	2.684387	1.405165	-7.3E-05
C	-1.67433	-0.10031	-8E-06
C	-2.28514	1.171272	-0.00013
H	-1.66975	2.063366	-0.00019
C	1.80602	0.43082	0.000004
C	-2.46015	-1.2657	0.00007
H	-1.96422	-2.23112	0.000161
C	-4.45763	0.093175	-8.7E-05
H	-5.54037	0.173589	-0.00012
C	-3.67231	1.258138	-0.00017
H	-4.15111	2.232407	-0.00026
C	-3.85145	-1.16696	0.000031
H	-4.45915	-2.06599	0.000091
C	4.045178	-0.3544	0.000114
H	4.988366	-0.88729	0.000177
N	3.972816	0.953094	-0.00001

Table S9. Cartesian coordinates of ground state optimized geometry of **h**.

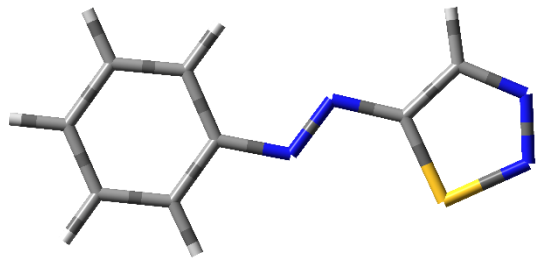

	X	Y	Z
S	-2.55314	-1.165	-0.00034
N	0.306049	-0.34703	-1.5E-05
N	-0.4353	0.678352	0.000073
C	1.69315	-0.11008	0.000036
C	2.290698	1.168009	0.000155
H	1.665882	2.053471	0.000217
C	-1.7902	0.394191	0.000011
C	2.492553	-1.26653	-4.6E-05
H	2.00753	-2.2375	-0.00014
C	4.47534	0.11407	0.00011
H	5.55714	0.20629	0.00014
C	3.676935	1.270077	0.00019
H	4.144886	2.24964	0.000281
C	3.882642	-1.15252	-8E-06
H	4.500008	-2.04499	-6.9E-05
N	-4.04743	0.857923	0.000038
C	-2.77943	1.359399	0.00004
H	-2.61342	2.428253	0.00012
N	-4.11789	-0.4285	0.000181

Table S10. Cartesian coordinates of ground state optimized geometry of **i**.

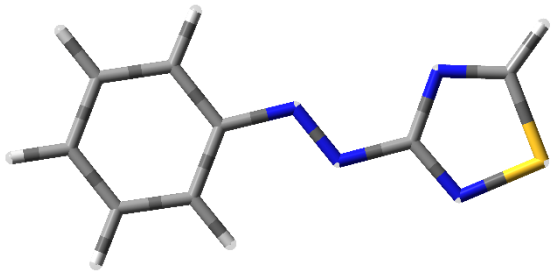

	X	Y	Z
N	-0.44461	0.512397	-0.00022
N	0.348842	-0.46608	-0.00016
C	-1.81851	0.178733	-5.2E-05
C	-2.32773	-1.13575	0.000202
H	-1.64294	-1.97568	0.000284
C	-2.69512	1.27611	-0.00016
H	-2.27808	2.278278	-0.00036
C	-4.5803	-0.23605	0.000227
H	-5.65333	-0.40207	0.000335
C	-3.70425	-1.33382	0.00034
H	-4.10342	-2.3435	0.000536
C	-4.0751	1.067591	-2.6E-05
H	-4.75164	1.916251	-0.00011
C	1.710049	-0.11057	-0.00011
S	4.110682	-0.46753	-0.00014
C	3.482801	1.152716	0.000116
H	4.118646	2.030883	0.000175
N	2.5721	-1.11495	0.000023
N	2.179211	1.186147	0.000094

Table S11. Cartesian coordinates of ground state optimized geometry of **j**.

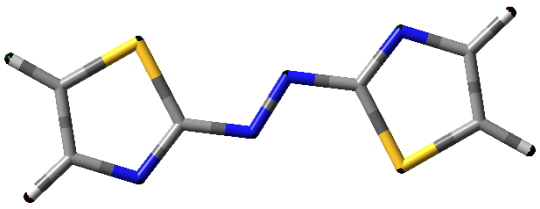

	X	Y	Z
S	-2.52796	1.198369	0.000272
N	0.335889	0.537808	0.000384
N	-0.3359	-0.53749	0.000167
N	-2.51085	-1.41169	-6.5E-05
C	-1.70601	-0.37063	0.000022
C	-3.8167	-1.01373	-0.00027
H	-4.60314	-1.75816	-0.00045
C	-4.02779	0.346179	-0.00036
H	-4.97294	0.872444	-0.00056

C	1.706014	0.37076	0.000581
S	2.527824	-1.19833	-0.00016
N	2.511141	1.411606	-0.0006
C	4.027659	-0.34642	0.000504
C	3.816836	1.013584	-0.00047
H	4.972711	-0.87286	0.000785
H	4.603479	1.757835	-0.00092

Table S12. Cartesian coordinates of ground state optimized geometry of **k**.

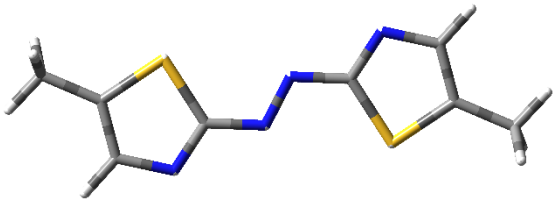

	X	Y	Z
S	-2.62123	0.975518	-0.00009
N	0.289711	0.5656	-2.2E-05
N	-0.28971	-0.56561	-2.3E-05
N	-2.38138	-1.62148	-6.6E-05
C	-1.66537	-0.51805	-0.00003
C	-3.71455	-1.33391	-0.00004
H	-4.43598	-2.14281	-4.2E-05
C	-4.06319	0.001637	0.000034
C	1.665366	0.518041	0.00003
S	2.621233	-0.97552	0.000135
N	2.381374	1.621474	0.000044
C	4.063185	-0.00164	-5.6E-05
C	3.714542	1.333907	0.000039
H	4.435971	2.142814	0.000014
C	-5.4372	0.591403	0.000107
H	-5.60237	1.216833	0.88387
H	-5.60243	1.216914	-0.88359
H	-6.1811	-0.20927	0.000096
C	5.437205	-0.59139	-0.00012
H	5.602489	-1.21673	0.883688
H	5.602321	-1.217	-0.88377
H	6.181096	0.209283	-0.00031

Table S13. Cartesian coordinates of ground state optimized geometry of **l**.

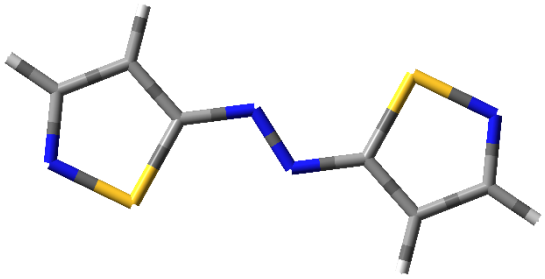

	X	Y	Z
S	2.560874	1.173354	-0.0005
N	-0.3371	0.537376	-5.7E-05
N	0.337274	-0.53743	0.000095
C	1.707072	-0.36015	0
C	2.622731	-1.39377	0.000035
H	2.353489	-2.44201	0.000158
N	4.075381	0.439538	-7E-06
C	3.94538	-0.878	0.000039
H	4.844412	-1.48576	0.000183
C	-1.70679	0.359821	0.000103
S	-2.56142	-1.17368	0.000046
C	-2.62218	1.39377	-4.8E-05
N	-4.07561	-0.43895	0.000606
H	-2.35266	2.441939	-0.00025
C	-3.94497	0.878434	0.00027
H	-4.84366	1.486712	0.000369

Table S14. Cartesian coordinates of ground state optimized geometry of **m**.

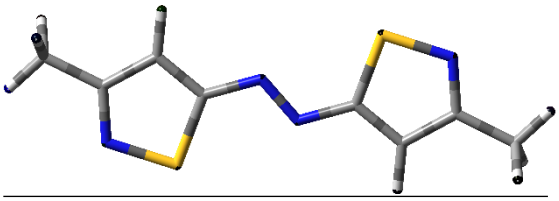

	X	Y	Z
S	-2.37216	-1.52057	-9.9E-05
N	0.408542	-0.48534	-0.00029
N	-0.40854	0.48532	-0.00018
C	-1.7406	0.118031	-0.00015

C	-2.78974	1.010548	0.000023
H	-2.66569	2.086103	0.000135
N	-3.975	-0.99731	-0.00044
C	-4.04368	0.326813	-0.00015
C	1.740604	-0.11804	-2.1E-05
S	2.372145	1.520566	0.00061
C	2.789746	-1.01055	0.000003
N	3.974995	0.997315	0.000157
H	2.66571	-2.08611	-0.0002
C	4.043684	-0.32681	0.000104
C	-5.37928	1.011205	-0.00017
H	-5.48336	1.65002	0.883296
H	-5.48292	1.650863	-0.88306
H	-6.18521	0.274936	-0.00071
C	5.379287	-1.01119	-2.1E-05
H	5.483344	-1.65019	0.883307
H	5.482951	-1.65066	-0.88305
H	6.185217	-0.27492	-0.00038

Table S15. Cartesian coordinates of ground state optimized geometry of **n**.

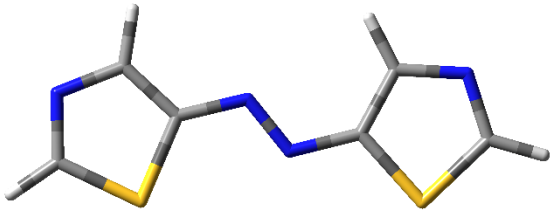

	X	Y	Z
S	-2.47329	-1.18903	-0.00021
N	0.351124	-0.23751	0.000021
N	-0.44478	0.753582	0.000057
C	-1.77928	0.435369	-4.1E-05
C	-4.0441	-0.44055	-0.0002
H	-4.93788	-1.05397	-0.00029
C	-2.7949	1.372304	-3.4E-05
N	-4.06824	0.871193	-0.00013
H	-2.62524	2.441947	0.000049
C	1.695472	0.096599	0.000094
S	2.864979	-1.20555	-1.4E-05
C	2.357504	1.31306	0.000215
C	4.123325	-0.01326	0.000234
N	3.721876	1.238335	0.00029
H	1.863039	2.27542	0.000276
H	5.165096	-0.31058	0.000271

Table S16. Cartesian coordinates of ground state optimized geometry of **o**.

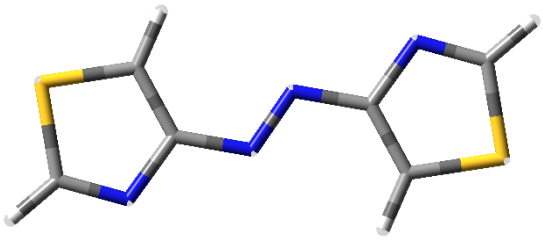

	X	Y	Z
N	-0.35869	-0.51935	0.00007
N	0.358721	0.519217	0
C	1.740259	0.278498	-4.5E-05
C	2.401203	-0.93383	-6.2E-05
N	2.551234	1.397581	-0.00018
S	4.098692	-0.67271	0.000149
C	3.805651	1.053778	-0.00033
H	4.632175	1.753924	-0.00044
H	1.967736	-1.92298	-3E-06
C	-1.74031	-0.27853	0.000029
C	-2.40124	0.933691	-0.00013
N	-2.55125	-1.39775	0.000063
S	-4.09868	0.672827	0.000157
H	-1.96768	1.922818	-0.00021
C	-3.80561	-1.0536	-0.00011
H	-4.63219	-1.75365	-0.00011

Table S17. Cartesian coordinates of ground state optimized geometry of **p**.

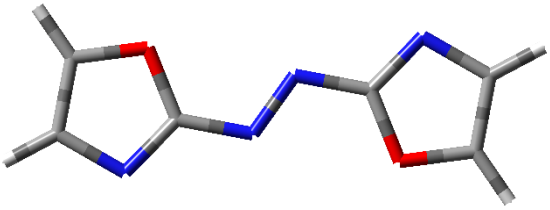

	X	Y	Z
N	0.369823	0.517108	0.000017
N	-0.36998	-0.5174	0.00009
C	1.718511	0.262581	0.000142
C	3.580285	-0.82896	0.000393
C	3.833326	0.515148	0.000295
H	4.191897	-1.71742	0.000543
H	4.787911	1.019499	0.000334
O	2.229697	-1.0039	0.000311
N	2.63865	1.198681	0.00006
C	-1.71855	-0.26267	-0.00011
O	-2.22954	1.003894	-0.00036
N	-2.63878	-1.19869	-7.5E-05
C	-3.58017	0.829127	-0.00048
C	-3.83332	-0.51496	-0.00028
H	-4.19165	1.717674	-0.00068
H	-4.78795	-1.01921	-0.00029

Table S18. Cartesian coordinates of ground state optimized geometry of **q**.

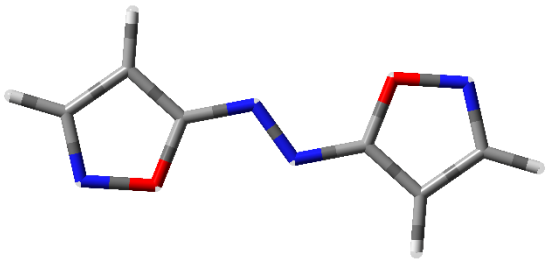

	X	Y	Z
N	-0.37091	0.515662	-4.8E-05
N	0.370841	-0.51547	-0.00013
C	-1.72418	0.25702	-0.00015
C	-3.91231	0.36622	-0.00014
H	-4.94974	0.673814	-0.0001
O	-2.22931	-1.00369	-0.00028
C	1.72413	-0.25695	0.000082
O	2.229423	1.003694	0.000371
C	3.91231	-0.36636	0.000422
H	4.949713	-0.67406	0.000546
N	-3.62461	-0.91962	-0.00047
N	3.624723	0.919492	0.000438
C	-2.74634	1.172314	-0.00016
H	-2.66258	2.247667	-0.00007
C	2.746229	-1.17231	0.000026
H	2.662365	-2.24765	-0.00018

Table S19. Cartesian coordinates of ground state optimized geometry of **r**.

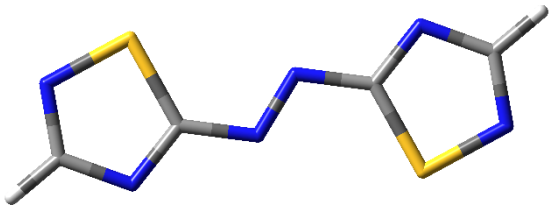

	X	Y	Z
S	-2.56218	1.167643	0.000343
N	0.326497	0.540181	-0.00019
N	-0.32645	-0.53996	-0.00025
N	-2.52164	-1.39368	0.000015
C	-1.70634	-0.36181	-0.00017
C	-3.80353	-0.93123	-8.7E-05
H	-4.63541	-1.62587	-0.00034
N	-4.03335	0.370463	-0.00049
C	1.706401	0.361802	-0.0001
S	2.562047	-1.16762	0.000307
N	2.521766	1.393652	0.000191
N	4.033262	-0.37059	-0.00046
C	3.803671	0.931122	0.000065
H	4.635626	1.625682	-0.00012

Table S20. Cartesian coordinates of ground state optimized geometry of **s**.

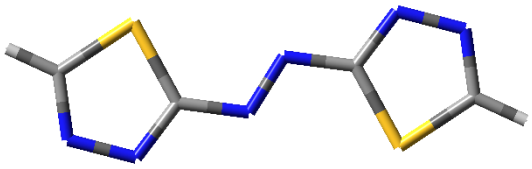

	X	Y	Z
S	-2.55404	1.189004	-0.00027
N	0.334216	0.535207	-0.00015
N	-0.33421	-0.53518	-0.00012
N	-2.50186	-1.40206	-0.00015
C	-1.70846	-0.35415	-0.00015
C	-3.99794	0.239687	-0.00025
H	-4.98218	0.69219	-0.00031
N	-3.81637	-1.06117	-0.00022
C	1.70846	0.354139	0.000075
S	2.553955	-1.18896	0.00034
N	2.501957	1.402026	0.000039
C	3.997905	-0.23974	0.000463
N	3.81648	1.061136	0.000256
H	4.982097	-0.69233	0.000647

Table S21. Cartesian coordinates of ground state optimized geometry of **t**.

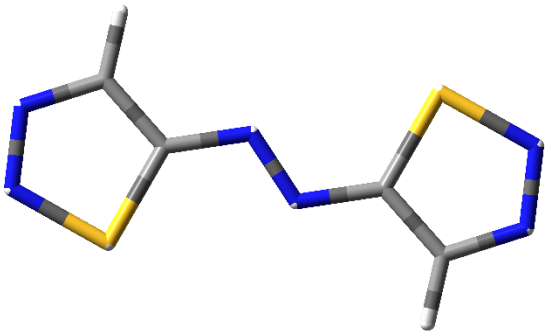

	X	Y	Z
S	2.580183	1.175195	-0.0003
N	-0.3468	0.52968	-8.6E-05
N	0.347091	-0.53046	0.000019
C	1.712995	-0.32648	-6.2E-05
N	3.929108	-0.94831	-8.8E-05
C	2.631079	-1.36143	0.000019
H	2.389793	-2.41587	0.000152
N	4.08383	0.33146	-0.00022
C	-1.71279	0.326071	0.000041
S	-2.58096	-1.17519	0.000298
C	-2.63033	1.361405	-4.8E-05
N	-4.08378	-0.33091	0.000327
N	-3.92866	0.948894	0.000105
H	-2.38867	2.415773	-0.00022

Table S22. Cartesian coordinates of ground state optimized geometry of **u**.

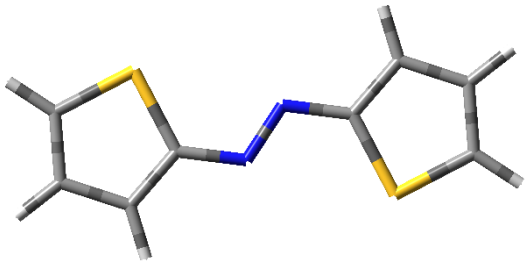

	X	Y	Z
N	0.348462	0.533463	0.000524
N	-0.3482	-0.53252	0.000508
C	1.710321	0.362381	0.000342
S	2.536443	-1.20454	-9.1E-05
C	4.076382	-0.40263	0.000509
C	3.966779	0.967972	0.000293
H	4.984012	-0.99236	0.000692
H	4.821889	1.633202	0.00036
C	2.616922	1.408466	0.0002
H	2.300937	2.444777	0.000214
C	-1.71006	-0.36201	0.000132
S	-2.53708	1.204605	-0.00081
C	-2.61634	-1.40841	-9.3E-05
C	-4.07655	0.40192	-0.00013
C	-3.96632	-0.96864	-0.00022
H	-2.29982	-2.44457	0.000075
H	-4.9844	0.991308	-0.00012
H	-4.82112	-1.63428	-0.00019

Table S23. Cartesian coordinates of ground state optimized geometry of **v**.

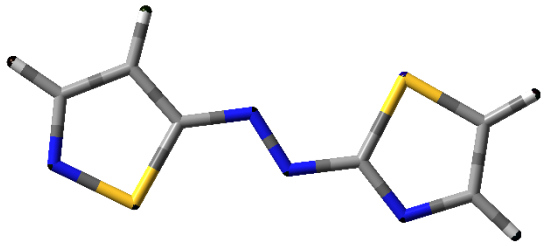

	X	Y	Z
N	-0.32266	0.532553	0.000011
N	0.351315	-0.54203	0.000016
C	-1.69173	0.357829	-0.0001
S	-2.54934	-1.17379	-0.00028
C	1.72241	-0.37255	0.000123
S	2.540774	1.19769	0.000177
C	4.042006	0.34869	0.000433
C	3.833924	-1.01185	0.000255
H	4.986107	0.876865	0.000601
H	4.62189	-1.75461	0.00029
C	-2.60585	1.393302	-0.00015
H	-2.33417	2.440867	-9.9E-05
N	-4.06298	-0.4371	-0.00025
N	2.528842	-1.41199	0.000094
C	-3.92936	0.880251	-0.00023
H	-4.82681	1.490425	-0.00024

Table S24. Cartesian coordinates of ground state optimized geometry of **w**.

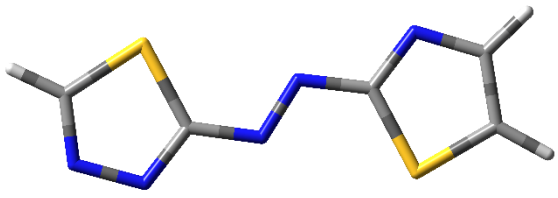

	X	Y	Z
S	2.530865	-1.19511	-0.00013
N	-0.34254	-0.54651	0.00008
N	0.328161	0.527199	0.000069
N	2.494247	1.415094	-5.7E-05
C	1.697776	0.36592	-3.5E-05
C	4.020173	-0.3327	-0.00024
H	4.969535	-0.85158	-0.00034
C	-1.71423	-0.36074	0.000155
S	-2.54778	1.192455	-0.00012
N	-2.51891	-1.39965	-0.00011
C	-4.00276	0.255595	0.000754
N	-3.83304	-1.04477	0.000127
H	-4.9827	0.717308	0.00093
C	3.800059	1.028575	-0.00018
H	4.582268	1.777261	-0.00022

Table S25. Cartesian coordinates of ground state optimized geometry of **x**.

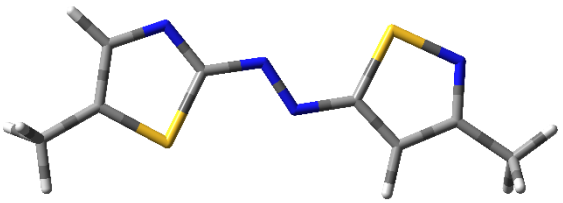

	X	Y	Z
S	-2.50512	-1.05252	-0.00041
N	0.349663	-0.32756	0.000114
N	-0.35371	0.730617	0.000069
C	-1.71544	0.532099	-5.7E-05
C	-3.84021	1.123837	-8.3E-05
C	1.712893	-0.11182	0.000089
S	2.523322	1.447355	-0.00012
C	2.658563	-1.11401	0.000092
N	4.060351	0.75032	0.000182
H	2.417696	-2.16962	0.00012
C	3.980151	-0.57302	0.000157
C	5.231295	-1.40259	0.000333
H	5.263068	-2.04912	0.883851
H	5.262848	-2.04986	-0.88264
H	6.114464	-0.7609	-2.9E-05
C	-4.04126	-0.24448	0.000088
N	-2.54864	1.55227	-0.00042

H	-4.64449	1.850487	0.000019
C	-5.34879	-0.97734	0.000399
H	-5.93469	-0.70698	0.885222
H	-5.93531	-0.70657	-0.88389
H	-5.21168	-2.0604	0.000104

11. References

[1]. G. M. Sheldrick, *Acta. Cryst*., **2015**, A71, 3–8.

[2]. G. M. Sheldrick, *Acta. Cryst*., **2015**, C71, 3–8.

[3]. O. V. Dolomanov, L. J. Bourhis, R. J. Gildea, J. A. K. Howard, H. Puschmann, *J. Appl. Cryst*., **2009**, 42, 339–341.

[4]. M. J. Frisch, G. W. Trucks, H. B. Schlegel, G. E. S.; M. A. Robb, J. R. Cheeseman, G. Scalmani, V. Barone, B. M.; G. A. Petersson, H. Nakatsuji, M. Caricato, X. Li, H. P. H.; A. F. Izmaylov, J. Bloino, G. Zheng, J. L. Sonnenberg, M. H.; M. Ehara, K. Toyota, R. Fukuda, J. Hasegawa, M. Ishida, T. N.; Y. Honda, O. Kitao, H. Nakai, T. Vreven, J. A. Montgomery, J.; J. E. Peralta, F. Ogliaro, M. Bearpark, J. J. Heyd, E. B.; K. N. Kudin, V. N. Staroverov, T. Keith, R. Kobayashi, J. N.; K. Raghavachari, A. Rendell, J. C. Burant, S. S. Iyengar, J. T.; M. Cossi, N. Rega, J. M. Millam, M. Klene, J. E. Knox, J. B. C.; V. Bakken, C. Adamo, J. Jaramillo, R. Gomperts, R. E. S.; O. Yazyev, A. J. Austin, R. Cammi, C. Pomelli, J. W. O.; R. L. Martin, K. Morokuma, V. G. Zakrzewski, G. A. V.; P. Salvador, J. J. Dannenberg, S. Dapprich, A. D. D.; O. Farkas, J. B. Foresman, J. V. Ortiz, J. C.; Fox., and D. J. Gaussian 09, Revision D.01. Gaussian, Inc., Wallingford CT **2013**.

[5]. Roy Dennington, Todd A. Keith, and J. M. M. GaussView, Version 6.1. Semichem Inc., Shawnee Mission, KS **2016**.

[6]. Hohenberg, P.; Kohn, W. Inhomogeneous Electron Gas. *Phys. Rev*. **1964**, 136 (3B), B864. https://doi.org/10.1103/PHYSREV.136.B864/FIGURE/1/THUMB. 97

[7]. Gross, E. K. U.; Dobson, J. F.; Petersilka, M. Density Functional Theory of Time-Dependent Phenomena. Density Funct. Theory II **1996**, 81–172. https://doi.org/10.1007/BFB0016643.

[8]. Kohn, W.; Sham, L. J. Self-Consistent Equations Including Exchange and Correlation Effects. *Phys. Rev*. **1965**, 140 (4A), A1133. https://doi.org/10.1103/PHYSREV.140.A1133/FIGURE/1/THUMB.

[9]. Lee, C.; Yang, W.; Parr, R. G. Development of the Colle-Salvetti Correlation Energy Formula into a Functional of the Electron Density. *Phys. Rev*. B **1988**, 37 (2), 785. https://doi.org/10.1103/PhysRevB.37.785.

[10]. Miertuš, S.; Scrocco, E.; Tomasi, J. Electrostatic Interaction of a Solute with a Continuum. A Direct Utilizaion of AB Initio Molecular Potentials for the Prevision of Solvent Effects. *Chem. Phys*. **1981**, 55 (1), 117–129. https://doi.org/10.1016/0301-0104(81)85090–2.